Collect. Vol. Sci. Pap. ICCAT, 82(3), SCRS/2025/050: 1-31 (2025)

SPATIO-TEMPORAL MODEL FOR CPUE STANDARDIZATION: APPLICATION TO WHITE MARLIN CAUGHT BY JAPANESE TUNA LONGLINE FISHERY FROM 1959 TO 2023

Mikihiko Kai[1]

SUMMARY

Abundance indices of white marlin caught by the Japanese tuna-longline fishery were estimated using logbook data from 1959 to 2023. The nominal CPUEs were standardized using the spatio-temporal generalized linear mixed model (GLMM) to provide the annual changes in the abundances. The author focused on spatial and interannual variations of the density in the model to account for spatiotemporal changes in the fishing location due to the target changes of tuna and tuna-like species. Based on the long-term changes in operational area and average weight of white marlin, the data was divided into four periods (P1: 1956-1977, P2: 1978-1992, P3: 1993-2013, P4: 2014-2023), and the CPUE was standardized for each period. The estimated annual CPUEs in P1 revealed a moderate increasing trend from 1959 to 1964 and then monotonically decreased until 1977. Those in P2, P3, and P4 revealed a slight decreasing trend. The estimated CPUE using the spatio-temporal model with a large amount of data collected in the wide area in the Atlantic Ocean is very useful information about the spatiotemporal changes in the abundance.

RESUMEN

Se estimaron los índices de abundancia de aguja blanca capturada por la pesquería japonesa de túnidos con palangre utilizando los datos de los cuadernos de pesca desde 1959 hasta 2023. Las CPUE nominales se estandarizaron mediante el modelo mixto lineal generalizado espaciotemporal (GLMM) para obtener los cambios anuales en las abundancias. El autor se centró en las variaciones espaciales e interanuales de la densidad en el modelo para dar cuenta de los cambios espaciotemporales en la localización de la pesca debidos a los cambios de especies objetivo de los túnidos y especies afines. Basándose en los cambios a largo plazo de la superficie operativa y el peso medio de la aguja blanca, los datos se dividieron en cuatro periodos (P1: 1956-1977, P2: 1978-1992, P3: 1993-2013, P4: 2014-2023), y la CPUE se estandarizó para cada periodo. Las CPUE anuales estimadas en P1 revelaron una tendencia creciente moderada de 1959 a 1964 y luego disminuyeron de forma monótona hasta 1977. Los de P2, P3 y P4 revelaron una ligera tendencia a la baja. La CPUE estimada utilizando el modelo espaciotemporal con una gran cantidad de datos recogidos en la amplia zona del océano Atlántico es una información muy útil sobre los cambios espaciotemporales en la abundancia.

RÉSUMÉ

Les indices d'abondance du makaire blanc capturé par la pêcherie palangrière thonière du Japon ont été estimés en utilisant les données des carnets de pêche de 1959 à 2023. Les CPUE nominales ont été standardisées à l'aide d'un modèle mixte linéaire généralisé spatio-temporel (GLMM) afin de fournir les changements annuels de l'abondance. L'auteur s'est concentré sur les variations spatiales et interannuelles de la densité dans le modèle afin de tenir compte des changements spatio-temporels de la localisation de la pêche en raison des changements de ciblage des thonidés et des espèces apparentées. Sur la base des changements à long terme de la zone opérationnelle et du poids moyen du makaire blanc, les données ont été divisées en quatre périodes (P1 : 1956-1977, P2 : 1978-1992, P3 : 1993-2013, P4 : 2014-2023), et la CPUE a été normalisée pour chaque période. Les CPUE annuelles estimées dans P1 ont révélé une tendance modérée à la hausse de 1959 à 1964, qui a ensuite diminué de façon constante jusqu'en 1977. Celles estimées dans P2, P3 et P4 ont montré une légère tendance à la baisse. La CPUE estimée en utilisant le modèle spatio-temporel avec une grande quantité de données collectées dans une large zone de l'océan Atlantique est une information très utile sur les changements spatio-temporels de l'abondance.

[1] Fisheries Resources Institute, Japan Fishery Research and Education Agency. 2-12-4, Fukuura Kanazawa, Yokohama, Kanagawa, Japan.

KEYWORDS

Atlantic white marlin, Kajikia akbida,
Japanese tuna longline, CPUE standardization, GLMM, spatio-temporal model

1. Introduction

The white marlin (*Kajikia akbida*) is a highly migratory species of billfish endemic to the Atlantic Ocean and this species is widely distributed from tropical to temperate waters in the Atlantic, however, mainly distributed in the subtropical and tropical waters (ICCAT 2024). The tropical western North and South Atlantic have historically been known as the primary spawning and feeding areas for this species, and spawning occurs during the spring-summer seasons. This species reaches a maximum size beyond 2.8 m in lower-jaw fork length and over 82 kg in weight (Nakamura 1985). This species is an epipelagic and oceanic species usually found in waters with surface temperatures greater than 22 ℃ (Nakamura 1985). This species is also known to exploring depths ranging from 0 to 387 m and experiencing temperatures ranging from 7.8 to 30 ℃, and they mostly spend in the upper 20 m of the water column for both day (50.8%) and night (81.6%) (Hoolihan et al. 2015). There are two main types of descent observed in this species. One pattern involves deep, V-shaped dives of relatively short duration (mean: 23.4 minutes), while the other consists of broader, U-shaped descent that remain at a specific depth range for an extended period (mean: 75.8 minutes) (Horodysky et al. 2007). These results appear that the white marlin directs a significant portion of their foraging efforts well below the surface waters. Since this species is a major bycatch of tuna longline fleets operating in the Atlantic Ocean targeting albacore (*Thunnus alalunga*), yellowfin tuna (*Thunnus albacares*), and bigeye tuna (*Thunnus obesus*), the behavior of vertical movement may explain the relatively high catch rates of white marlin on some deep-set LL deployments.

The white marlin (*Kajikia albida*) appears morphologically similar to the Indo-Pacific striped marlin (*Kajikia audax*). However, they are distinguishable by slight differences in the shape of the dorsal and pectoral fins (Nakamura 1985). Nevertheless, genetic studies had failed to resolve white marlin and striped marlin as separate lineages for several decades. Collette et al. (2006) presented genetic evidence to propose a taxonomic reclassification of the white marlin and the Indo-Pacific striped marlin into the genus *Kajikia*. Until 2006, the white marlin and the Indo-Pacific striped marlin were known by the accepted names *Tetrapturus albidus* and *Tetrapturus audax* because the white marlin is morphologically similar to the longbill spearfish (*Tetrapturus pfluegeri*) and the roundscale spearfish (*Tetrapturus georgii*). Now, the white marlin and the Indo-Pacific striped marlin have been scientifically determined to be genetically distinct from the species in the genus *Tetrapturus*. The difficulty in species identification lowers the reliability in the records of logbook data. As a matter of fact, the catch ratio of roundscale spearfish in the western Atlantic was estimated to be between 23% and 27% (ICCAT 2024).

The benchmark stock assessment for the white marlin was conducted in 2019 using two assessment models (Bayesian surplus production model: JABBA, and stock synthesis: SS3) with fishery data for 1956-2017 (ICCAT 2024). Both models estimated similar annual trends of biomass and fishing mortality, although the initial depletion of biomass from JABBA was lower than that from SS3 and the fishing mortality in 1990s from JABBA was significantly higher than that from SS3. The combined Kobe plots for the final base cases of JABBA and SS3 model indicated that the stock is overfished but not undergoing overfishing. The probability of being in the yellow quadrants of the Kobe plot was estimated to be 99 % and that of being in the green quadrant less than 1%. The Commission established a landing limit of 335 t in 2019 [Rec. 19-05]. Landing in 2023 was below the limit in Rec. 19-05.

In the previous benchmark stock assessment in 2019, Japan provided standardized CPUEs (catch per unit effort) of white marlin caught by Japanese tuna longline fishery operating in the Atlantic Ocean from 1976 to 2017. The annual CPUEs were estimated based on Japanese logbook data using a zero-inflated generalized linear mixed model (GLMM) assuming a Poisson error distribution (Ijima and Honda 2019). In the analysis, logbook data was separated into three periods: Early period (1976-1993), Middle period (1994-2000), and Late period (2001-2017). The reason for not using data prior to 1976 is that hooks between floats (HBF) information is fully available from 1975 onwards, and vessel information is only available from 1976 onwards. Additionally, the reason for dividing the period after 1993 is that the format of logbook data changed after 1993, significantly increasing the information on fishing gear, such as gear materials and the length of branch lines. The reason for dividing the period after 2000 is that management measures [Rec. 19-05] regarding the reporting of live release for white marlin were introduced in 2001 (ICCAT 2024). In addition, the spatial area used in the CPUE standardization was limited to the eastern Atlantic in the tropical area between 10°S and 20°N, where subadult and adult white marlins (with a mean semi-

dressed body weight of approximately 30 kg) were mainly caught from 1994 to 2017 (**Figure A1**). The first predictor of the best model included year and quarter as fixed effects. The second predictor of the best model included area effect, vessel effect, and gear effect (i.e., HBF) as random effects, in addition to the fixed effects of year and quarter. Annual changes in the standardized CPUEs showed a decreasing trend throughout all periods. However, the analysis has some issues because (1) the main interaction terms such as a "year-area" effects were not included in the model, (2) the negative binomial model was not used as the error distribution, although the count data indicated the overdispersion, (3) although it is a reasonable idea to use the core area of subadult and adult white marines, the areas with high CPUE of this species were spread across a wide region of the western Atlantic, and designating a part of the eastern Atlantic as the core area does not necessarily indicate the abundance indices, and (4) The information on CPUE standardization from 1959 to 1975, presented in the 2012 stock assessment (Yokawa et al. 2001), was not updated. The abundance index for this period provides useful information on the early depletion of the stock due to fisheries development and offers important data for estimating virgin biomass (B0) and the initial fishing mortality (F).

The VAST (Vector Autoregressive Spatio-Temporal) software package for R (Thorson 2019), which enables us to analyze fishery data using the spatio-temporal GLMM (Thorson et al. 2015), is commonly used globally to estimate spatial changes in species distribution and temporal variations in a population range and density. The basic model structure of VAST adopts a delta-GLMM which can consider spatio-temporal correlations among categories such as species (Thorson et al. 2017) and length frequency (Kai et al. 2017). This spatiotemporal model can utilize to overcome the above issues and improve the CPUE standardization by adding functions such as random effects for the interaction terms as well as assuming the error distribution as a negative binomial model.

The objective of this working paper is to estimate the standardized CPUE of white marlin caught by Japanese tuna longline fishery operating in the Atlantic Ocean for 1959-2023 using the spatio-temporal GLMM in consideration with spatial and temporal changes in the density.

2. Materials and Methods

2.1 Data sources

Set-by-set logbook data from Japanese tuna longline fisheries in the Atlantic Ocean, which is available from 1959, were used to estimate the annual standardized CPUEs of white marlin in the area for 1959-2023. The logbook data includes information about date of operation, catch number/catch weight of tuna and tuna-like species and bycatch species such as sharks and billfishes, amount of effort (number of hooks), number of HBF as a proxy for gear configuration, location/station/cell (longitude and latitude) of set by resolution of 1 × 1 degree square, and vessel identity (vessel name/call sign/license number).

2.2 Data filtering and separation

The logbook data in the Atlantic Ocean were filtered to remove unrealistic or unsuitable records and separated into categorical datasets for appropriate analysis.

1. The set-by-set data from the Mediterranean and areas other than the Atlantic Ocean were removed.
2. The set-by-set data where the catch number of white marlins was unavailable (i.e., NA) was removed.
3. The set-by-set data were divided into four seasons: Spring (April-June), Summer (July-September), Autumn (October-December), and Winter (January-March).
4. The set-by-set data were separated into four periods (P1: 1956-1977, P2: 1978-1992, P3: 1993-2013, P4: 2014-2023) based on long-term changes in operational patterns (**Figure 1**) and average weight, which is available from 1971 (**Figure A2**).
5. The set-by-set data with the number of HBF, available from 1975, between 3 and 30 were used for each dataset of the three periods (P2, P3, and P4) to remove unrealistic records on the gear settings.
6. The set-by-set data in the operation area (**Figure 1**) where latitude and longitude zones with low catch numbers of white marlins were removed for each period:
    - P1: South of 43°S, North of 45°N, West of 98°W, and East of 19°E
    - P2: South of 41°S, North of 44°N, West of 81°W, and East of 19°E
    - P3: South of 41°S, North of 44°N, West of 81°W, and East of 19°E
    - P4: South of 35°S, North of 22°N, West of 45°W, and East of 12°E
7. The set-by-set data for each vessel, where the license number is available from 1975, that had no catch of white marlin were removed for each period (P2, P3, and P4).

2.3 Catchability covariate

Except for the station's effect, the nominal CPUEs of white marlin were largely influenced by year, quarter, vessel, number of HBF, and target change (**Figure A3**). In the Atlantic Ocean, Japanese longline fisheries change the target species by altering the operational area, gear configuration, season, etc. The number of HBF was used to identify target change through changes in the depth of hook distribution (Bigelow et al. 2006). Cluster analysis based on k-means clustering of observed catch proportions for tunas, swordfish, and/or billfishes (Carvalho et al. 2010; Chang et al. 2011) was used to identify target species. The issue of multicollinearity was evaluated using correlations among quarters, number of HBF, cell/station, and cluster for four periods (**Figure A4**). Some high correlations were observed in combination with the station, but high correlations were not seen in other combinations. Vessel name was treated as a random effect to account for individual differences in vessel catchability. Since the available covariates and their quality vary by period, the covariate settings were slightly adjusted for each period (**Table 1**).

2.4 CPUE standardization with spatio-temporal model

The spatio-temporal model (Thorson 2019) consists of two components: encounter probability and positive catch in a delta model. Although the encounter probability of white marlin is low (mean values were 38%, 8.9%, 4.9%, and 2.4% for P1, P2, P3, and P4, respectively), the first predictor was fixed at an estimated constant value because the annual trends in the positive catch ratio and those in the nominal CPUE were almost the same throughout all periods (**Figure 2**). This means that multiplying the two predictors would cause large variance without reflecting actual annual trends in abundance. The second predictor was modeled using a Negative Binomial (NB) model to account for the count data, where the mean dispersion ratio was 27.88%, 7.71%, 3.28%, and 1.78% for P1, P2, P3, and P4, respectively:

$$\begin{aligned} &c \sim NegBin\ (c^*, c^*(1+\sigma_1) + c^{*2}\sigma_2), \\ &\log\ (d) = d_0(t) + \gamma(s) + \theta(s,t) + \epsilon(v) + \textstyle\sum_{j=1}^{n_j} \beta_j x_j, \end{aligned} \quad (1)$$

where c is observed catch, $NegBin\ (a, b)$ is a negative binomial distribution with mean a and variance b (Lindén and Mäntyniemi 2011), c^* is an expected catch and a function of density d and fishing effort f(number of hooks = 1), σ_1 and σ_2 are residual variations, $d_0(t)$ represents temporal variation (the intercept for each year t), $\gamma(s)$ represents spatial variation (s), $\theta(s,t)$ represents spatio-temporal variation (station s and year t), $\epsilon(v)$ represents random variation in catchability for the vth vessel, and β_j represents the impact of covariate j with value x_j on catchability. The targeting cluster, the three-month quarters, and the number of hooks between floats (i.e. $n_j = 3$, $x_j = l, q, and\ h$) are used as covariates (changing the catchability) corresponding to Eq. (1).

The VAST (version VAST_v14_0_0) software package for R (Thorson, 2019) was applied to standardize the nominal CPUE of white marlin in the Atlantic Ocean from 1959 to 2023. The annual abundance index relative to the average $\hat{I}$ was estimated as:

$$\hat{I}(t) = \textstyle\sum_{s=1}^{n_s} f(s) \times d(s,t) / \{\sum_{t=1}^{n_t} \sum_{s=1}^{n_s} f(s) \times d(s,t)\}, \quad (2)$$

where n_s is total number of knots and f is fishing effort at location s. Different numbers of knots (500, 100, 100, and 300 locations) were given for P1, P2, P3, and P4, respectively. The number of knots was adjusted according to the quality and quantity of the data.

2.5 Model selection and diagnostics

To select the best model, the explanatory variable was sequentially added to both predictors of the simple null model (Model-0). The best model was selected using BIC (Schwarz 1978) because AIC (Akaike 1973) tends to choose complex models with a lot of data (Shono 2005). For the best model, the goodness of fit was examined using Pearson residuals and QQ-plot. The residuals were computed using a randomized quantile (Dunn and Smyth 1996) to produce continuous normal residuals. The Poisson model was also applied to the selected model for P4 because the dispersion ratio was low (1.78%). However, the negative binomial model was selected based on the BIC (the results of the Poisson model are not shown in this paper).

3. Results

3.1 Summary of data filtering and basic annual trends

The data filtering based on the number of HBF, positive catch ratio of each vessel, and operational area reduced the number of records for this analysis from 1,411,840 sets to 1,020,282 sets (P1: 221,772 sets; P2: 300,276 sets; P3: 431,821 sets; and P4: 66,413 sets). Annual catch numbers, number of hooks, nominal CPUE, and positive catch ratio for this species before and after data filtering are shown in **Figure 2**. Annual catches of white marlin were almost the same before and after data filtering. The annual catch of striped marlin peaked at approximately 100,000 fish in 1965, but then sharply declined from the late 1960s to the early 1970s, dropping to less than 10,000 fish by 1977. During the 1980s, the catch fluctuated between 2,000 and 6,000 fish, and since the 1990s, it has gradually decreased further, falling below 1,000 fish after 2014. The levels of annual fishing effort, annual nominal CPUE, and annual positive catch ratio for P2, P3, and P4 significantly changed after data filtering. However, those trends were almost similar before and after data filtering, while those for P1 were slightly changed due to limited data filtering because of the lack of information about HBF and vessel names. Annual fishing effort showed a gradual increase since 1959, peaking in 1996, and has consistently decreased thereafter. The nominal CPUE and positive catch ratio showed similar annual trends. Both increased sharply after 1959, peaked between 1963 and 1966, then sharply declined until the early 1970s. Thereafter, they continued to decrease until around 2014, after which they stabilized at low levels.

3.2 Selection of the best model

All models except Model-0 for P4 reasonably converged with a positive definite Hessian matrix and a small maximum gradient (< 0.001) (**Table 2**). The saturated models (Model-4 for P1, Model-5 for P2, Model-6 for P3, and Model-5 for P4) include spatial (station/cell) and spatio-temporal variance (year and station) and variation over vessel effects (vessel effect was not included in Model-4 for P1) as random effects. The effects of cluster, quarter, and HBFs (only Model-6 for P3) as fixed effects were identified by BIC as the most parsimonious model (**Table 2**). The estimated CPUE changed substantially when random effect components were sequentially added to the simple model, which had no random effects (Model-0) (**Figure 3**). The fixed effect components of quarter and cluster had a small effect to the annual trends in the CPUE (**Figure 3**), but they decreased the values of BIC (**Table 2**). The fixed effect component of HBF increased the BIC for Model-6, P2, and P4. Lists of all parameters and estimates of the best models are shown in **Table 3**.

3.3 Annual trends in CPUE

The estimated annual CPUEs in P1 revealed a moderate increasing trend from 1959 to 1964, peaking in 1965 then monotonically decreased until 1977 (**Figure 4.1**). Those in P2 revealed a slight decreasing trend, while annual fluctuations were observed (**Figure 4.2**). Those in P3 revealed a significant increase in 1994, followed by a slight decreasing trend, while annual fluctuations were observed (**Figure 4.3**). Those in P4 revealed a slight decreasing trend (**Figure 4.4**). The coefficient of variation (CV) for the CPUEs was larger after 2013 (**Figure 4**) due to a reduction in fishing effort and shrinkage of operational area, which limited the fishing area to the offshore waters of west Africa in the central and south Atlantic Ocean (**Figure A5**).

3.4 Model diagnostics

Diagnostic plots of goodness-of-fit for the best model of the four models didn't show a serious deviation from normality and model misspecification (**Figure 5**). These results suggested that the fittings of the best model to the data were good.

3.5 Spatial maps of estimated CPUE

The annual spatial maps of estimated CPUEs clearly showed higher CPUEs of white marlin in the western Atlantic (**Figure 6**). The areas of high estimated CPUE (i.e., hotspots) are observed in the northwestern Atlantic Ocean, including Gulf of Mexico, offshore Florida, the central Atlantic Ocean, including the Caribbean Sea, and the southern Atlantic Ocean, including offshore waters of west Africa, northeast Brazil, and Uruguay.

4. Discussions

This paper estimated the historical trend in abundance indices of white marlin caught by the Japanese tuna longline fishery in the Atlantic Ocean from 1959 to 2023 in order to provide the abundance indices for the upcoming benchmark stock assessment in 2025. The author applied spatio-temporal GLMM after separating the logbook data into four periods (i.e., 1959-1977, 1978-1992, 1993-2013, and 2014-2023) based on long-term changes in the operational pattern and average weight of white marlin. The advantages of the current analysis over the previous one are: (1) the main interaction term of a "year-area" effect was used in the model as the random effects, (2) the negative binomial model was used as the error distribution instead of Poisson model, (3) The definition of core area was reviewed and changed into the possible entire area including the western Atlantic Ocean, and (4) updated the CPUE of the early period from 1959 to 1975.

For the CPUE standardization of white marlin, it is crucial to consider the significant changes in operation pattern in terms of gear configuration and main fishing ground for Japanese longline fleets over time (Uozumi and Nakano 1994, Yokawa and Uozumi 2000) due to the target changes and fishing regulations. The fishing grounds in the North Atlantic gradually expanded from the tropical regions to the Gulf of Mexico and the Northwest Atlantic off the coasts of the United States and Canada in the 1960s and 1970s (**Figure A5**). The fishing grounds in the South Atlantic also expanded from off the coasts of Brazil and Uruguay to off the coasts of Namibia and South Africa in the same periods. The expansion of the operational area is due to changes in the target species from yellowfin tuna, albacore, and swordfish to bigeye, bluefin, and southern bluefin tuna (**Figure A6**). The relatively large number of billfishes caught during this period suggests that Japanese vessels were primarily engaged in shallow-set longline operations. By the mid to late 1970s, the fishing grounds are clearly divided into tropical-subtropical areas for targeting bigeye tuna and temperate areas for targeting bluefin tuna and southern bluefin tuna (**Figure A5**). The changes in the gear configurations (i.e., number of HBFs) from shallow-set to deep-set in the 1980s also support the large shifts of the target species (**Figure A7**). From the 1980s onwards, operations off the coast of west Africa became prominent, and from the 1990s to the 2000s, the bluefin tuna fishing grounds expanded, but due to fishing regulations, the fishing areas gradually shrank around 2007 (**Figure A5**). The high-density areas of white marlin in the high latitude of North Atlantic and Central American waters had almost disappeared after 2013. The operations of Japanese fleets are limited to the South Atlantic and offshore water off Africa since 2014. In the 2000s, due to the decline in the stock abundance of bigeye tuna, the proportion of yellowfin and albacore in total catch has increased (ICCAT 2024).

Seasonal changes in operational areas suggest that seasonal effects should be considered in CPUE standardization, like cluster analysis (**Figure A8**). Consequently, the author included the seasonal effect in the model.

By analyzing the historical changes in the operational areas of Japanese fleets, it becomes clear that these vessels have gradually moved away from areas with high densities of white marlin (**Figure A5**). In the current analysis, not only were these area changes considered, but also the average weight information was used to divide the periods. The average weight was calculated by dividing the total catch weight by the number of fish caught per operation. Unless there are extreme numbers of small or large individuals, the average weight serves as a rough indicator of individual size. It is evident that the average weight varied significantly across different periods and operational areas, suggesting that the selectivity for white marlin likely differed greatly by period and area. Therefore, it is reasonable to divide the analysis into four periods to account for changes in target species and fishing grounds. In the previous analysis, the core area was limited to tropical regions (**Figure A1**), which was due to the reduction in operational areas and the capture of larger individuals in this area since 1994 (Ijima and Honda 2019). However, applying this to all periods before 1994 is not considered appropriate.

The main advantage of the spatio-temporal model for the CPUE standardization is the imputation of missing data using spatial and temporal correlations through random effects (Thorson 2019). Compared to previous analyses (Yokawa et al. 2001, Kimoto and Yokawa 2012, Ijima and Honda 2019), this study incorporated the interaction between time and space as a random effect, allowing for a thorough examination of the impact of spatiotemporal changes. Although the data showed a high zero catch ratio of white marlin, the author did not consider encounter probability in the GLMM because the fact that most catches of white marlin are only a few individuals per operation. On the other hand, examining the dispersion ratio reveals that the mean and variance are not the same, with the variance being larger than the mean, indicating overdispersion in all periods. Although overdispersion has significantly decreased in recent years due to the decline in stock abundance, the NB model was chosen over the Poisson model for the P4 period, suggesting that the NB model is appropriate for the error distribution.

Yokawa et al. (2001) attempted to apply alternative approach (Hinton and Nakano, 1996) to the CPUE standardization of white marlin in the Atlantic Ocean using behavioral constraints of white marlin and environmental data. They concluded that the estimated annual CPUE is too early to use for the stock assessment because necessary data such as the vertical distribution of white marlin and hooking depth and time are insufficient to estimate precisely the CPUE. The author agreed that it is unnecessary to use the Hinton and Nakano's approach as for this analysis because Japan has not enough data to apply the approach.

The author recommends using the estimated annual CPUEs of white marlin caught by Japanese tuna longline fishery in the Atlantic Ocean for four periods from 1959 to 2023 as a representative of abundance indices in the Atlantic Ocean due to a wide coverage of the main distributional areas (tropical to temperate waters) of white marlin over time, sufficient long time series of data, and statistical soundness of the spatio-temporal model.

References

Akaike, H. 1973. Information theory and an extension of the maximum likelihood principle. *In* Petrov, B.N., Csaki, F. (Eds.) Second International Symposium on Information Theory, Budapest, Akademiai Kiado, pp 267–281.

Bigelow, K. Musyl, M.K. Poisson, F. and Kleiber, P. 2006. Pelagic longline gear depth and shoaling. Fish. Res. 77: 173–183. https://doi.org/10.1016/j.fishres.2005.10.010

Carvalho, F.C. Murie, D.J. Hazin, F.H.V. Hazin, H.G. Leite-mourato, B. Travassos, P. and Burgess, G.H. 2010. Catch rates and size composition of blue sharks (*Prionace glauca*) caught by the Brazilian pelagic longline fleet in the southwestern Atlantic Ocean. Aquat. Living Resour. 23: 373–385. https://doi.org/10.1051/alr/2011005

Chang, S.K. Hoyle, S. and Liu, H.I. 2011. Catch rate standardization for yellowfin tuna (*Thunnus albacares*) in Taiwan's distant-water longline fishery in the Western and Central Pacific Ocean, with consideration of target change. Fish. Res. 107(1-3): 210–220. https://doi.org/10.1016/j.fishres.2010.11.004

Collette, B.B. McDowell. J.R. and Graves, J.E. 2006. Phylogeny of recent billfishes (Xiphioidei). B. Mar. Sci. 79: 455–468.

Dunn, K.P. and Smyth, G.K. 1996. Randomized quantile residuals. J. Comput. Graph. Stat. 5(3): 236–244.

Hoolihan, J.P. Luo, J. Snodgrass, D. Orbesen, E.S. Barse, A.M. and Prince, E.D. Vertical and horizontal habitat use by white marlin *Kajikia albida* (Poey, 1860) in the western North Atlantic Ocean. ICES Journal of Marine Science, doi: 10.1093/icesjms/fsv082.

Horodysky, A.Z. D.W. Kerstetter, R.J. Latour and J.E. Graves. 2007. Habitat utilization and vertical movements of white marlin (Tetrapturus albidus) released from commercial and recreational fishing gears in the western North Atlantic Ocean: inferences from short duration pop-up archival satellite tags. Fish. Oceanogra. 16: 240-256.

ICCAT. 2024. Report of the standing committee on research and statistics (SCRS), Madrid, Spain. pp. 124–132.

Ijima, H. and Honda, H. 2019. Japanese longline CPUE standardization (1976-2017) for Atlantic white marlin (*Kajikikia albidus*) using zero-inflated generalized linear mixed model (GLMM). SCRS/2019/037.

Kai, M. Thorson, J.T. Piner, K.R. and Maunder, M.N. 2017. Spatiotemporal variation in size-structured populations using fishery data: an application to shortfin mako (*Isurus oxyrinchus*) in the Pacific Ocean. Can. J. Fish Aquat. Sci. 74(11): 1765–1780.

Kimoto, A. and Yokawa, K. 2012. Standardized CPUE of white marlin caught by Japanese longliners in the Atlantic Ocean using GLM model. Collect. Vol. Sci. Pap. ICCAT, 68(4): 1458-1469.

Lindén, A. and Mäntyniemi, A. 2011. Using the negative binomial distribution to model overdispersion in ecological count data. Ecology 92, 1414−1421.

Nakamura, I. 1985. FAO species catalogue. Vol. 5. Billfishes of the world. An annotated and illustrated catalogue of marlins, sailfishes, spearfishes and swordfishes known to date. FAO Fish. Synop. 125(5):65p. Rome: FAO.

Schwarz, G. 1978. Estimating the dimension of a model. Ann. Stat. 6(2): 461–464.

Shono, H. 2005. Is model selection using Akaike's information criterion appropriate for catch per unit effort standardization in large samples? Eish. Sci. 71: 978−986.

Thorson, J.T. 2019. Guidance for decisions using the Vector Autoregressive Spatio-Temporal (VAST) package in stock, ecosystem, habitat and climate assessments. Fish. Res. 210, 143−161.

Thorson, J.T. Fonner, R. Haltuch, M.A. Ono, K. and Winker, H. 2017. Accounting for spatiotemporal variation and fisher targeting when estimating abundance from multispecies fishery data. Can. J. Fish Aquat. Sci. 74(11): 1794−1807.

Thorson, J.T. Shelton, A.O. Ward, E.J. and Skaug, H. 2015. Geostatistical delta-generalized linear mixed models improve precision for estimated abundance indices for West Coast groundfishes. ICES J. Mar. Sci. 72(5): 1297−1310.

Uozumi, Y. and Nakano, H. 1994. A historical review of Japanese longline fishery and billfish catches in the Atlantic Ocean. Col. Vol. Sci. Pap. ICCAT, 41: 233-243.

Yokawa, K. and Uozumi, Y. 2001. Analysis of operation pattern of Japanese longliners in the tropical Atlantic and their blue marlin catch. Col. Vol. Sci. Pap. ICCAT, 53: 318–336.

Yokawa, K. Takeuchi, Y. Okazaki, M. and Uozumi, Y. 2001. Standardizations of CPUE of blue marlin and white marlin caught by Japanese longliners in the Atlantic Ocean. Collect. Vol. Sci. Pap. ICCAT, 53: 345–355.

Table 1. Summary of catchability coefficients used in the model for white marlin.

Period	Vessel effect	Number of species used in cluster analysis	Number of HBF
P1: 1959-1977	Not available	Five species (BET, YFT, ALB, BIL, and SWO)	Not available
P2: 1978-1992	Yes	Five species (BET, YFT, ALB, BFT, and SWO)	3~14, and 15~20
P3: 1993-2013	Yes	Four species (BET, YFT, ALB, and BFT)	3~14, and 15~25
P4: 2014-2023	Yes	Three species (BET, YFT, and ALB)	8~14, and 15~23

Table 2. Summary of model structure and outputs among different models for white marlin. All models include fixed effects. "Δ" denotes a difference between the value of criteria and the minimum value.

P1: 1959-1977

Model	Catch rate predictors of random effect	Number of parameters	Deviance	BIC	ΔBIC	Maximum gradient
0	Year	22	682728	682999	114139	< 0.0001
1	Year + Station	26	602605	602925	34065	< 0.0001
2	Year + Station + Year and Station	27	569461	569794	934	< 0.0001
3	Year + Station + Year and Station + Cluster	31	569301	569682	822	< 0.0001
4	Year + Station + Year and Station + Cluster + Quarter	34	568442	568860	0	< 0.0001

P2: 1978-1992

Model	Catch rate predictors of random effect	Number of parameters	Deviance	BIC	ΔBIC	Maximum gradient
0	Year	18	258394	258621	51242	< 0.001
1	Year + Station	22	223403	223681	16301	< 0.0001
2	Year + Station + Year and Station	23	216219	216510	9130	< 0.0001
3	Year + Station + Year and Station + Vessel	24	207606	207909	530	< 0.001
4	Year + Station + Year and Station + Vessel + Cluster	28	207584	207937	557	< 0.0001
5	Year + Station + Year and Station + Vessel + Cluster + Quarter	31	206988	207379	0	< 0.0001
6	Year + Station + Year and Station + Vessel + Cluster + Quarter + HBF	32	206982	207386	6	< 0.0001

P3: 1992-2013

Model	Catch rate predictors of random effect	Number of parameters	Deviance	BIC	ΔBIC	Maximum gradient
0	Year	24	216840	217152	203324	< 0.0001
1	Year + Station	28	191608	191971	178143	< 0.0001
2	Year + Station + Year and Station	29	184046	184423	170595	< 0.0001
3	Year + Station + Year and Station + Vessel	30	173483	173872	160044	< 0.0001
4	Year + Station + Year and Station + Vessel + Cluster	33	173471	173899	160071	< 0.0001
5	Year + Station + Year and Station + Vessel + Cluster + Quarter	36	173230	173697	159869	< 0.0001
6	Year + Station + Year and Station + Vessel + Cluster + Quarter + HBF	37	173167	173647	0	< 0.0001

P4: 2014-2023

Model	Catch rate predictors of random effect	Number of parameters	Deviance	BIC	ΔBIC	Maximum gradient
1	Year + Station	17	16581	16770	2942	< 0.0001
2	Year + Station + Year and Station	18	15623	15823	1995	< 0.0001
3	Year + Station + Year and Station + Vessel	19	13865	14076	248	< 0.0001
4	Year + Station + Year and Station + Vessel + Cluster	21	13842	14075	247	< 0.0001
5	Year + Station + Year and Station + Vessel + Cluster + Quarter	24	13562	13828	0	< 0.0001
6	Year + Station + Year and Station + Vessel + Cluster + Quarter + HBF	25	13561	13839	11	< 0.0001

Table 3. List of all parameters and estimates of the selected models (Model-4 for P1, Model-5 for P2, Model-6 for P3, and Model-5 for P4) for white marlin.

No	Parameter name	Symbol	Type	Estimates (P1)	Estimates (P2)	Estimates (P3)	Estimates (P4)
1	Distance of correlation (Spatial random effect)	κ	Fixed	0.0021	0.0018	0.0017	0.0043
2	Variation over vessel	σ_ϵ	Fixed		0.39	3.20	6.09
3	Northings anisotropy	h_1	Fixed	1.19	1.61	1.10	1.22
4	Anisotropic correlation	h_2	Fixed	0.95	1.08	0.93	0.71
5	Parameter governing pointwise variance (Spatial random effect)	η_γ	Fixed	2.70	9.49	0.20	0.47
6	Parameter governing pointwise variance (Spatio-temporal (year) random effect)	η_θ	Fixed	4.53	7.16	0.20	3.50
7	Residual variation 1 of negative binomial model	σ_1	Fixed	1.44	0.58	0.48	0.35
8	Residual variation 2 of negative binomial model	σ_2	Fixed	0.51	1.52	0.82	0.24
9	Coefficient of cluster 2	β_1	Fixed	0.80	0.98	1.01	0.74
10	Coefficient of cluster 3	β_2	Fixed	1.01	0.99	0.96	0.93
12	Coefficient of cluster 4	β_3	Fixed	0.98	0.90	1.07	
13	Coefficient of cluster 5	β_4	Fixed	1.00	1.01		
14	Coefficient of three-month quarters 2	β_5	Fixed	1.45	1.09	1.15	4.53
15	Coefficient of three-month quarters 3	β_6	Fixed	1.41	1.76	0.99	2.53
16	Coefficient of three-month quarters 4	β_7	Fixed	1.45	1.19	1.37	1.05
17	Coefficient of number of hooks between floats	β_8	Fixed			0.80	
18	Intercept for year	d_0	Fixed	Not shown	Not shown	Not shown	Not shown
19	Vessel effect	ϵ	Random	Not shown	Not shown	Not shown	Not shown
20	Spatial residuals	γ	Random	Not shown	Not shown	Not shown	Not shown
21	Spatio-temporal (year) residuals	θ	Random	Not shown	Not shown	Not shown	Not shown

Table 4. Summary of annual CPUE estimated by spatio-temporal model along with corresponding estimates of the coefficient of variation (CV), annual nominal CPUE, and number of hooks in millions for white marlin. Values are estimated using the best fitting model (Model 4 for P1, Model 5 for P2, Model 6 for P3, and Model 5 for P4) and CPUEs are scaled by average CPUE. Grey shade and white denotes the each time periods.

Year	Predicted CPUE	Nominal CPUE	CV	Number of hooks (millions)
1959	0.58	0.44	0.44	7.57
1960	0.18	0.42	0.17	15.63
1961	0.62	1.12	0.13	21.57
1962	1.32	1.62	0.13	33.47
1963	2.02	2.10	0.09	22.99
1964	2.07	2.48	0.04	30.66
1965	2.74	2.43	0.33	31.63
1966	2.01	2.62	0.09	12.37
1967	1.43	1.15	0.07	27.30
1968	1.27	1.15	0.15	21.45
1969	0.92	0.76	0.09	20.01
1970	0.93	0.59	0.09	29.82
1971	0.64	0.53	0.07	44.68
1972	0.65	0.28	0.14	29.89
1973	0.34	0.30	0.15	25.60
1974	0.41	0.30	0.17	25.19
1975	0.33	0.21	0.17	44.18
1976	0.35	0.41	0.17	29.65
1977	0.20	0.09	0.25	27.43
1978	1.63	1.00	0.30	19.26
1979	0.96	0.95	0.40	25.78
1980	1.10	1.18	0.33	43.40
1981	1.85	1.36	0.21	53.21
1982	1.09	0.98	0.29	62.48
1983	0.64	0.61	0.23	36.71
1984	0.79	0.70	0.24	49.79
1985	0.63	0.92	0.13	54.18
1986	1.02	1.20	0.20	44.08
1987	0.80	1.55	0.14	36.32
1988	1.45	1.12	0.78	58.52
1989	0.41	1.00	0.11	78.12
1990	0.65	0.85	0.18	76.96
1991	1.01	0.76	0.28	68.72
1992	0.97	0.81	0.25	61.57
1993	1.61	1.52	0.17	78.83
1994	3.52	1.31	0.37	78.93
1995	1.18	0.84	0.21	75.60
1996	1.03	1.53	0.19	85.53
1997	0.99	0.86	0.21	76.49
1998	1.19	0.85	0.21	64.31
1999	0.75	0.87	0.15	54.60
2000	1.62	1.46	0.20	56.27
2001	1.27	0.95	0.20	46.98
2002	0.25	0.42	0.19	40.43
2003	0.53	0.88	0.14	49.42
2004	0.46	0.82	0.13	52.32
2005	0.46	0.92	0.17	48.35
2006	0.98	0.91	0.24	49.09
2007	0.57	0.42	0.24	47.50
2008	1.32	0.64	0.32	54.31
2009	0.82	1.06	0.18	53.17
2010	0.90	0.96	0.32	57.98
2011	0.71	1.48	0.14	52.87
2012	0.46	1.30	0.25	49.57
2013	0.38	0.99	0.22	34.62
2014	2.14	0.93	0.32	22.89
2015	1.06	0.80	0.32	23.31
2016	1.06	1.04	0.33	22.92
2017	1.13	1.10	0.31	25.60
2018	0.84	0.65	0.31	24.72
2019	1.88	1.35	0.30	21.20
2020	0.64	1.06	0.30	21.82
2021	0.31	1.04	0.33	18.90
2022	0.33	0.62	0.41	11.16
2023	0.60	1.41	0.36	15.65

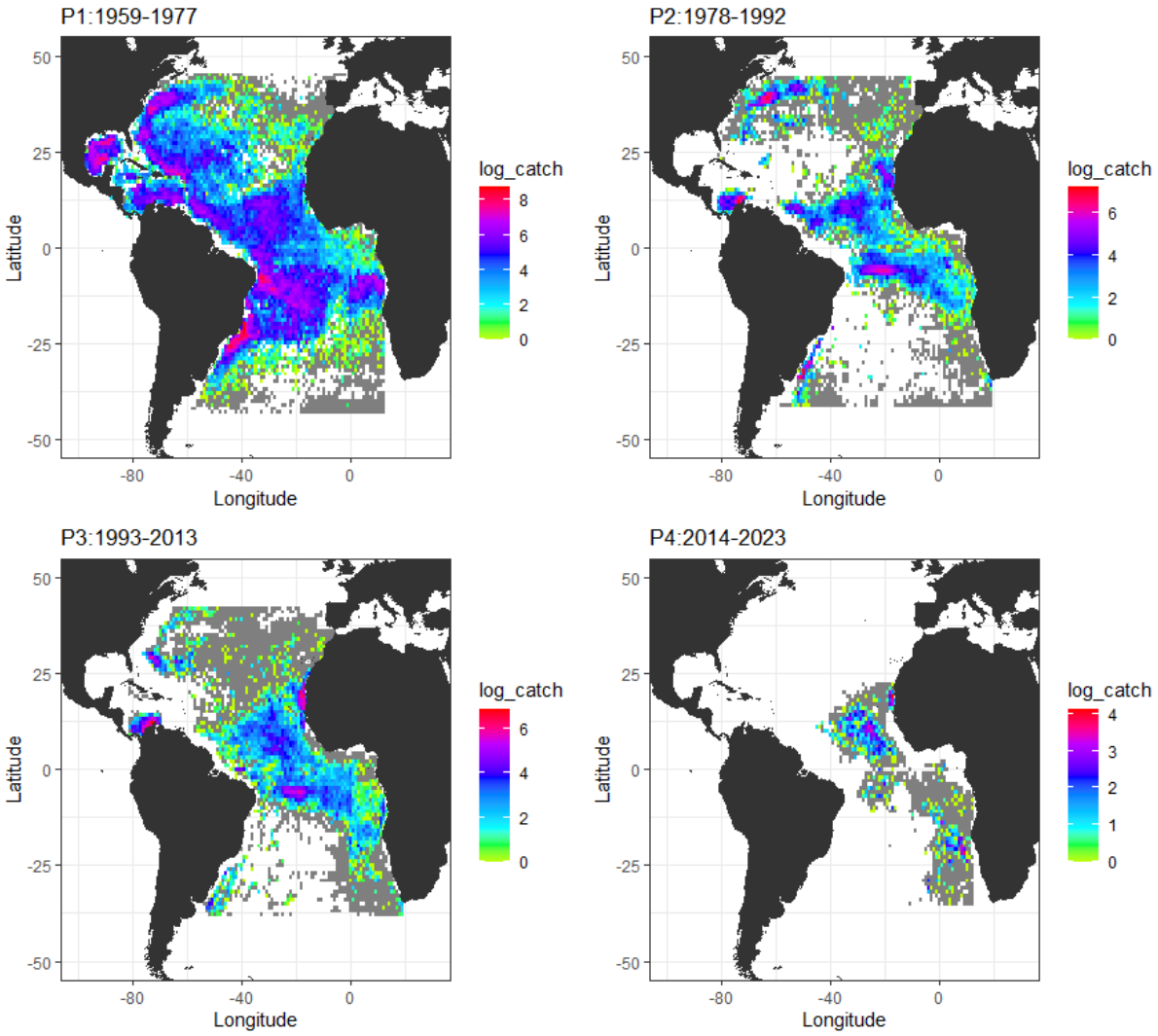

Figure 1. Spatial distribution of white marlin (log-scale of total catch in number) caught by Japanese longline fleet in the Atlantic Ocean for four periods (P1: 1959-1977, P2: 1978-1992, P3: 1993-2013, and P4: 2014-2023) after data filtering. Grey tile denotes zero catch.

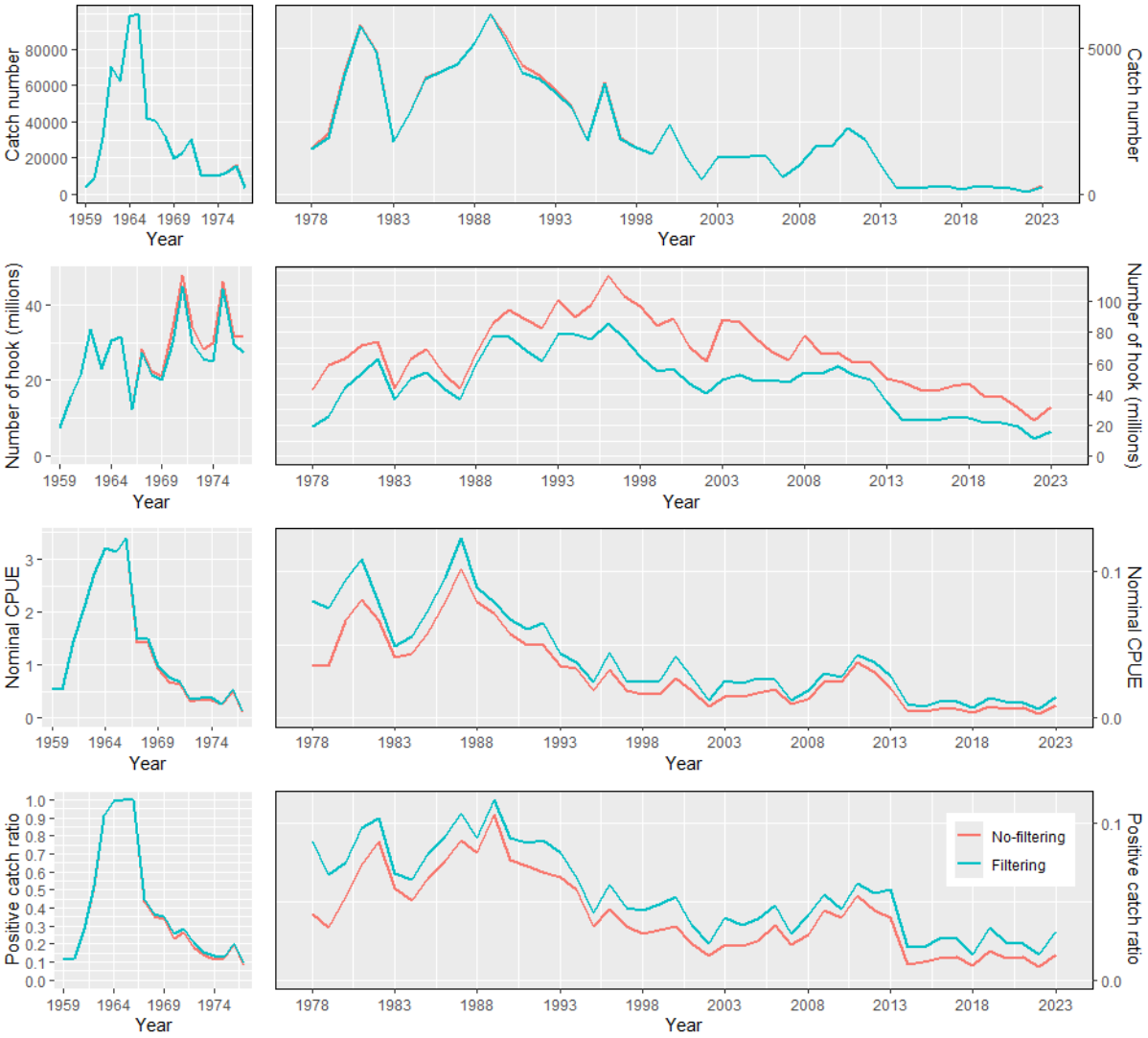

Figure 2. Annual catch in numbers, number of hooks (millions), nominal CPUE (per 1000 hooks), and positive catch ratio for white marlin in the Atlantic Ocean before and after data filtering from 1959 to 2023.

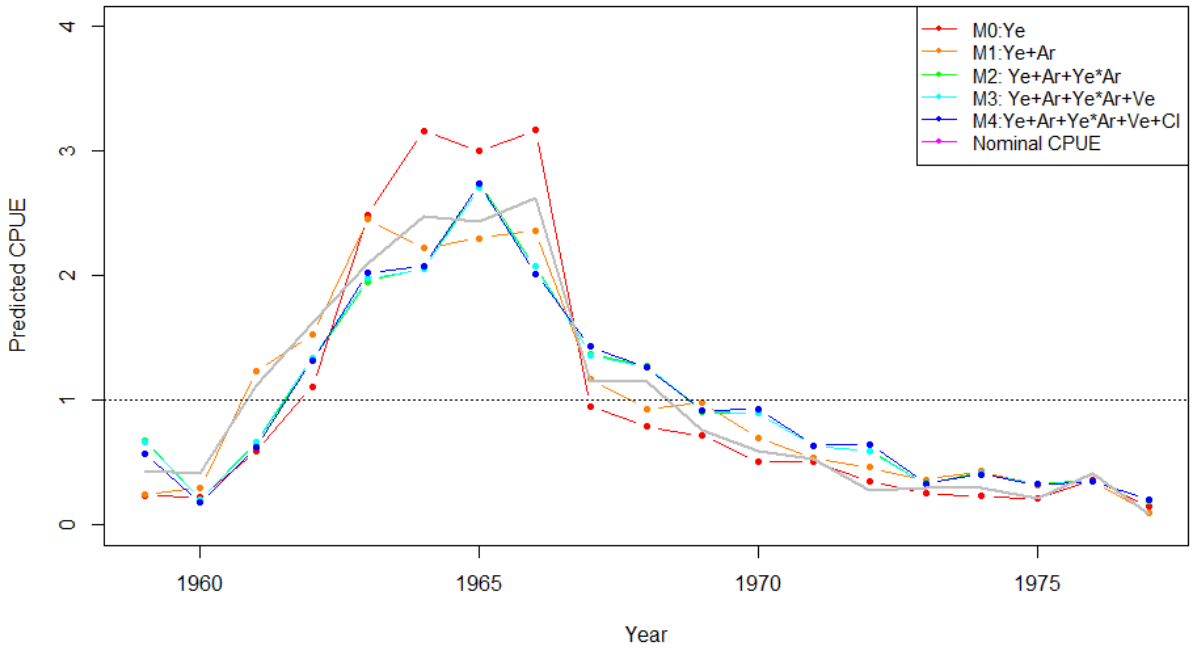

Figure 3.1 Comparisons of annual estimated CPUE relative to its average among different structures of the spatio-temporal model for white marlin in the Atlantic Ocean for P1 (1959-1977). For details of the models, see table 2.

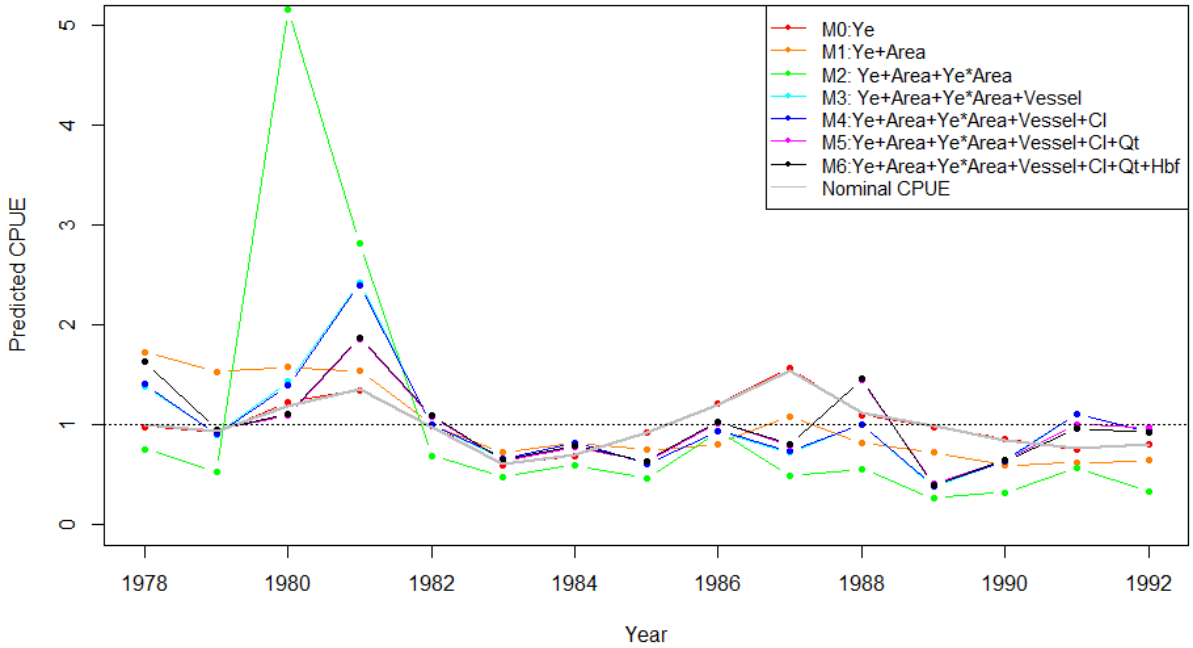

Figure 3.2 Comparisons of annual estimated CPUE relative to its average among different structures of the spatio-temporal model for white marlin in the Atlantic Ocean for P2 (1978-1992). For details of the models, see table 2.

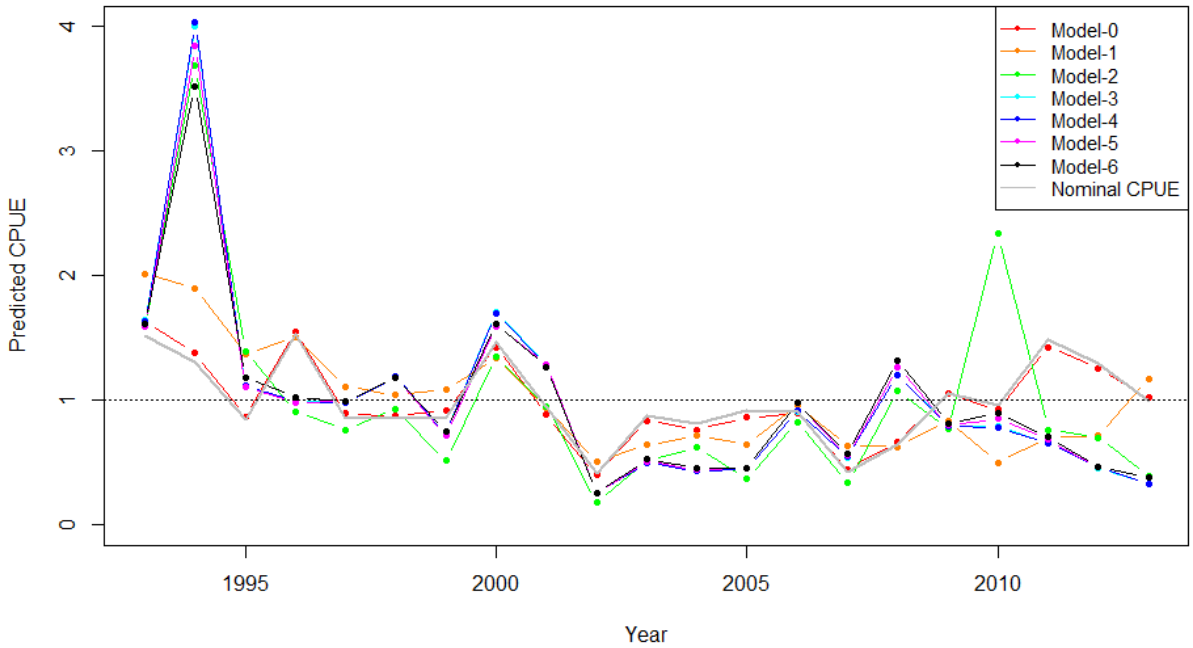

Figure 3.3 Comparisons of annual estimated CPUE relative to its average among different structures of the spatio-temporal model for white marlin in the Atlantic Ocean for four periods for P3 (1993-2013). For details of the models, see table 2.

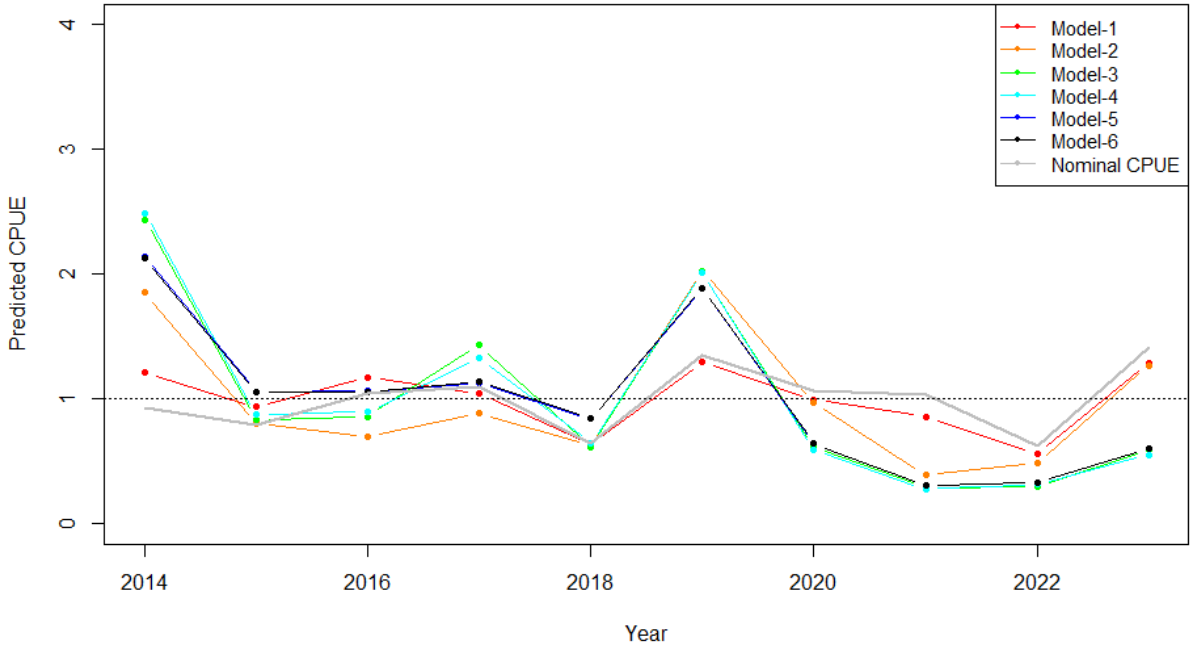

Figure 3.4 Comparisons of annual estimated CPUE relative to its average among different structures of the spatio-temporal model for white marlin in the Atlantic Ocean for four periods for P4 (2014-2023). For details of the models, see table 2.

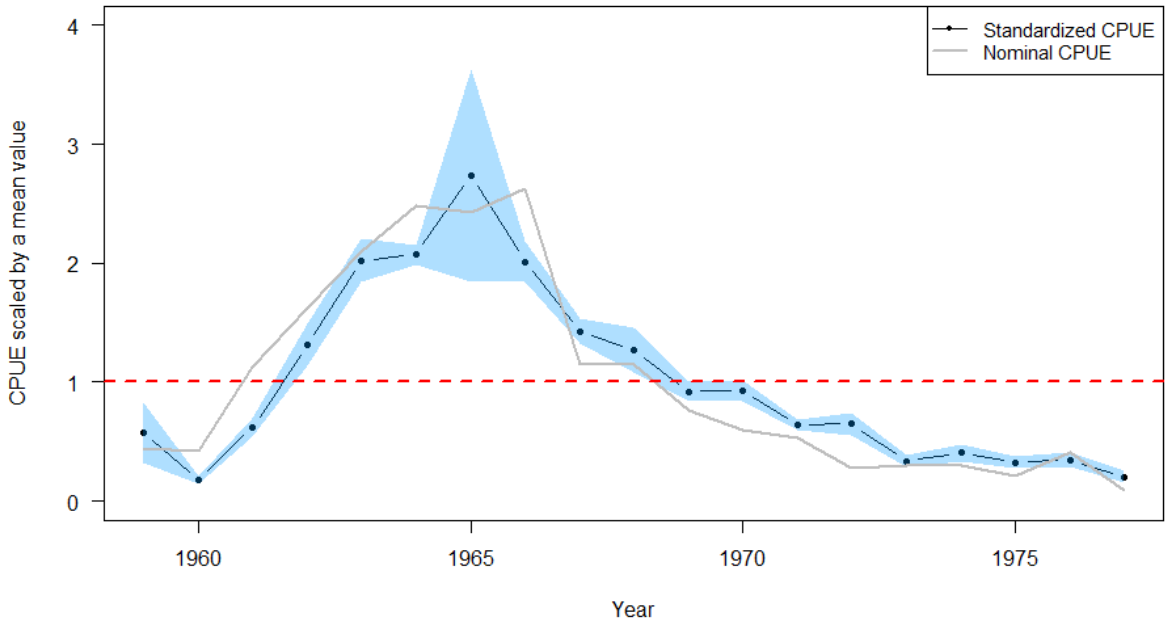

Figure 4.1 Annual estimated CPUE relative to its average for white marlin in the Atlantic Ocean for P1 (1959-1977). Gray solid line denotes nominal CPUE relative to its average, shadow denotes standard deviations, and horizontal red broken line denotes mean of relative values (1.0).

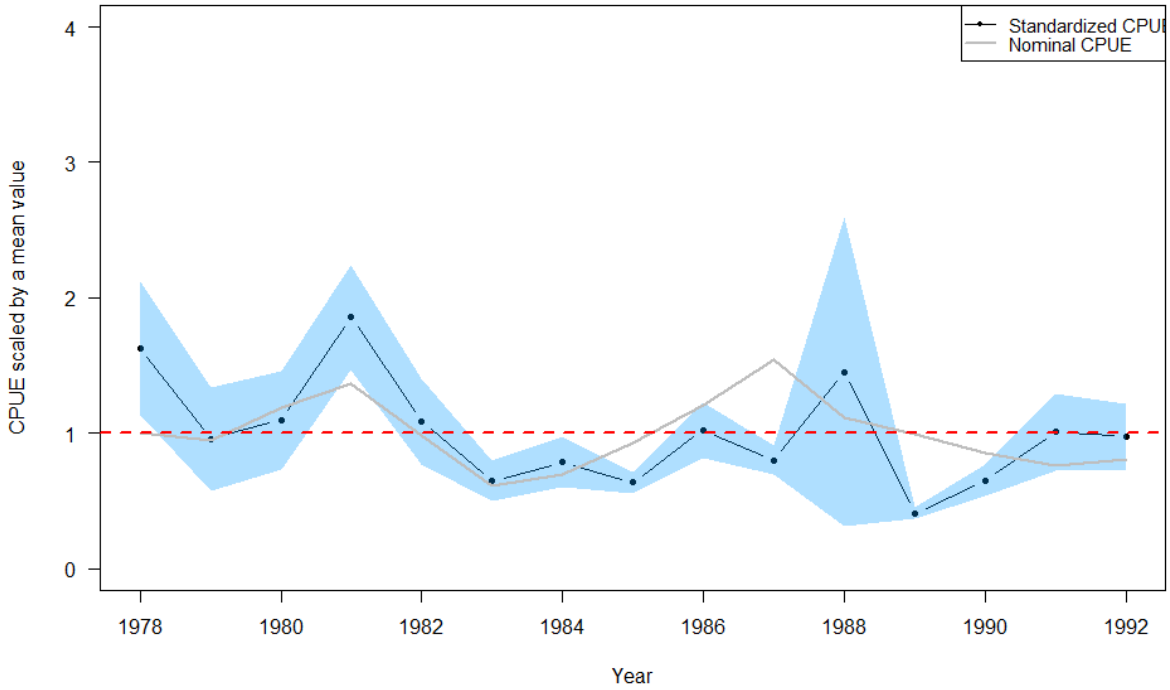

Figure 4.2 Annual estimated CPUE relative to its average for white marlin in the Atlantic Ocean for for P2 (1978-1992). Gray solid line denotes nominal CPUE relative to its average, shadow denotes standard deviations, and horizontal red broken line denotes mean of relative values (1.0).

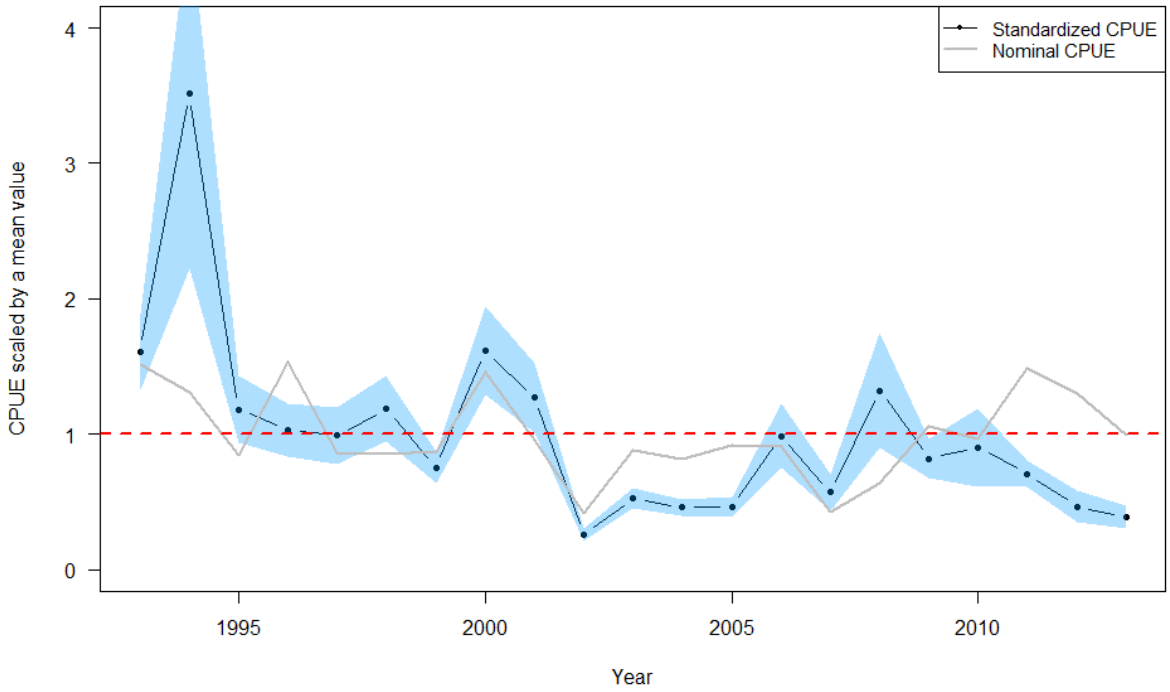

Figure 4.3 Annual estimated CPUE relative to its average for white marlin in the Atlantic Ocean for P3 (1993-2013). Gray solid line denotes nominal CPUE relative to its average, shadow denotes standard deviations, and horizontal red broken line denotes mean of relative values (1.0).

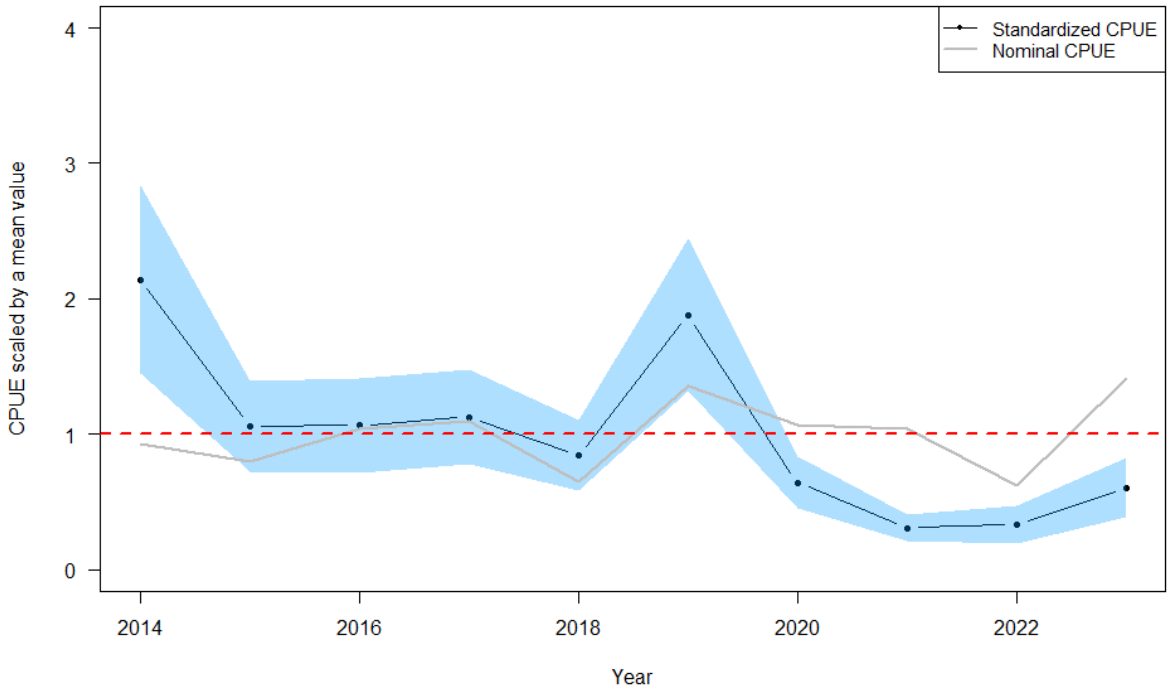

Figure 4.4 Annual estimated CPUE relative to its average for white marlin in the Atlantic Ocean for P4 (2014-2023). Gray solid line denotes nominal CPUE relative to its average, shadow denotes standard deviations, and horizontal red broken line denotes mean of relative values (1.0).

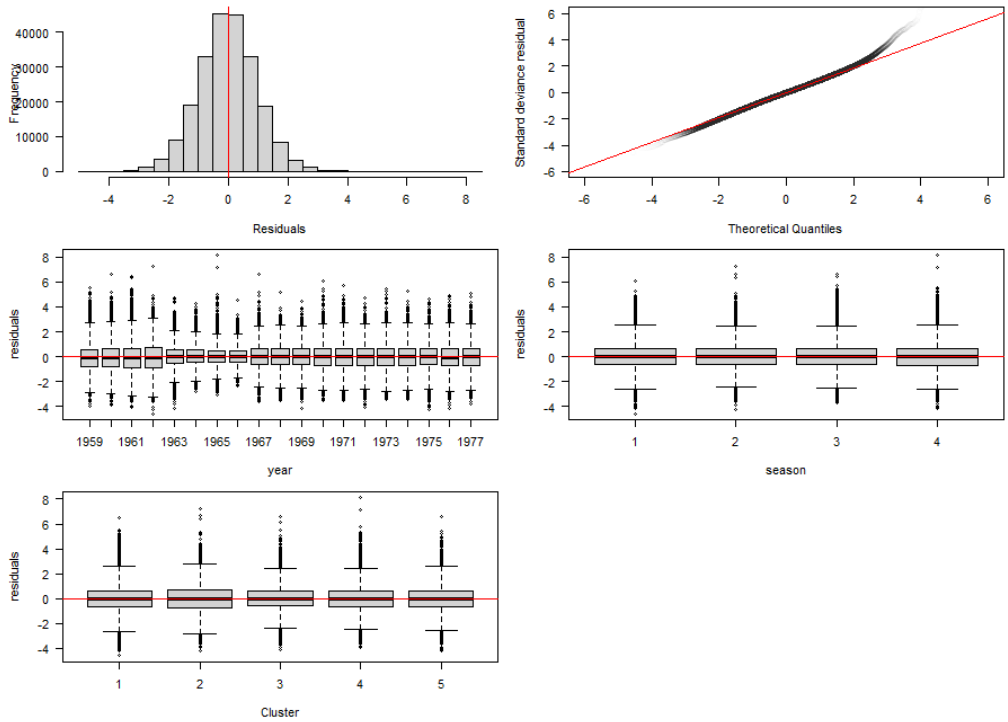

Figure 5.1 Diagnostic plots of goodness-of-fit for the most parsimonious model (Model-4) for white marlin in the Atlantic Ocean for P1(1959-1977).

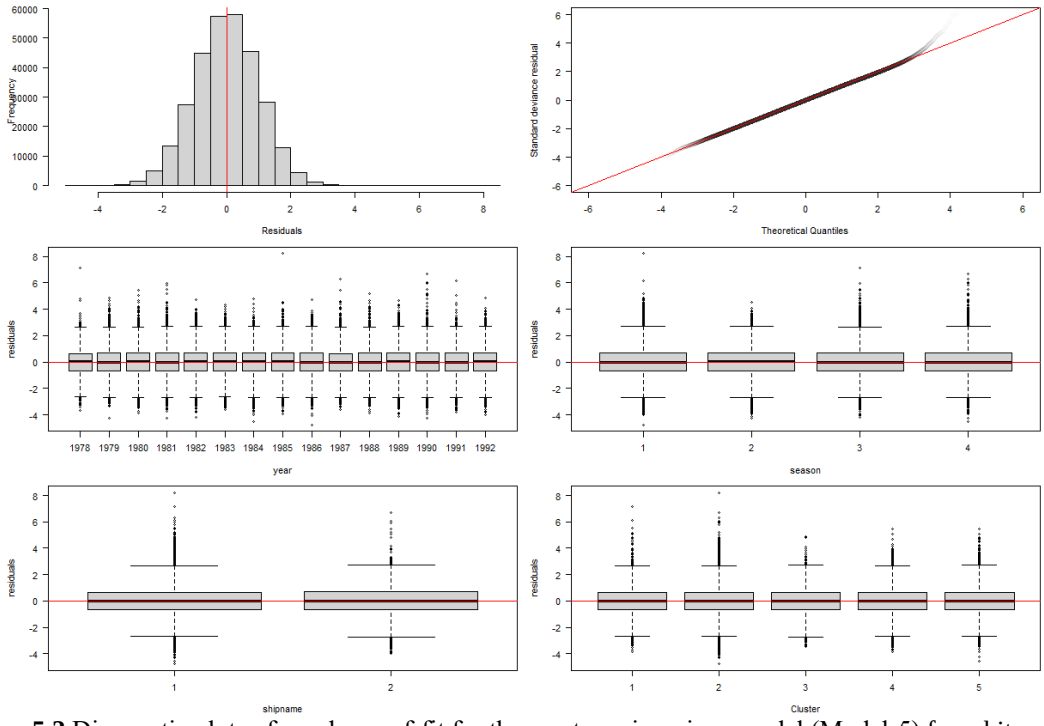

Figure 5.2 Diagnostic plots of goodness-of-fit for the most parsimonious model (Model-5) for white marlin in the Atlantic Ocean for P2 (1978-1992).

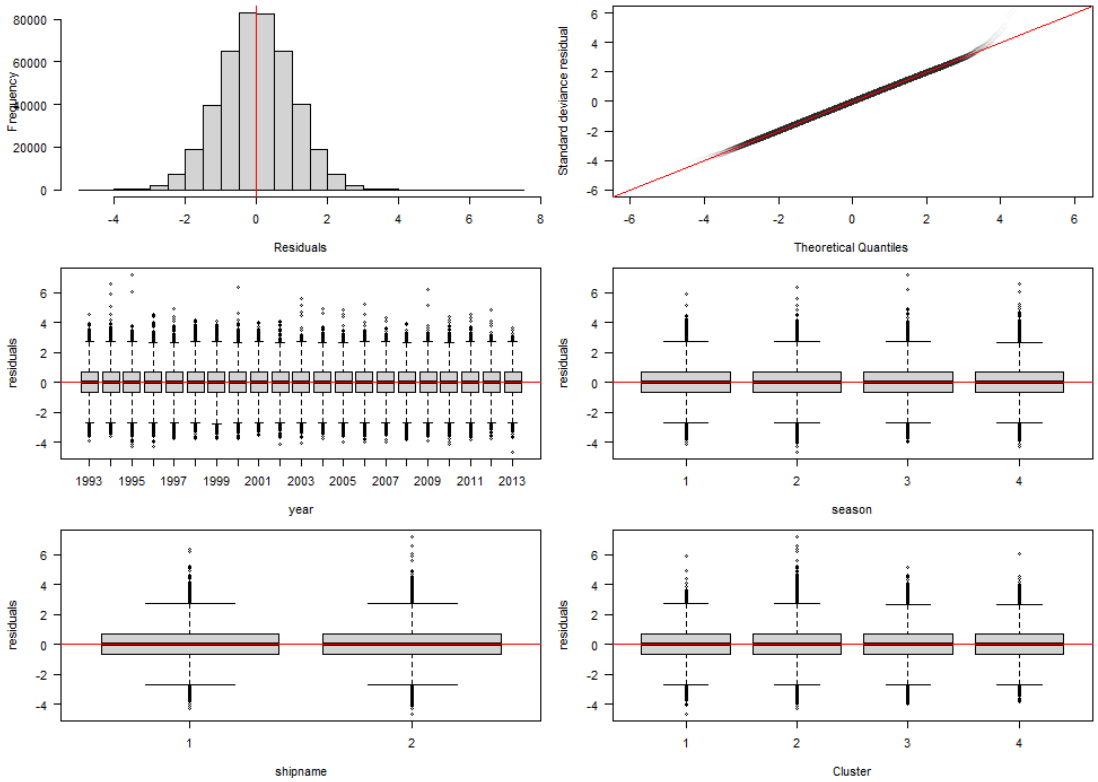

Figure 5.3 Diagnostic plots of goodness-of-fit for the most parsimonious model (Model-6) for white marlin in the Atlantic Ocean for P3 (1993-2013).

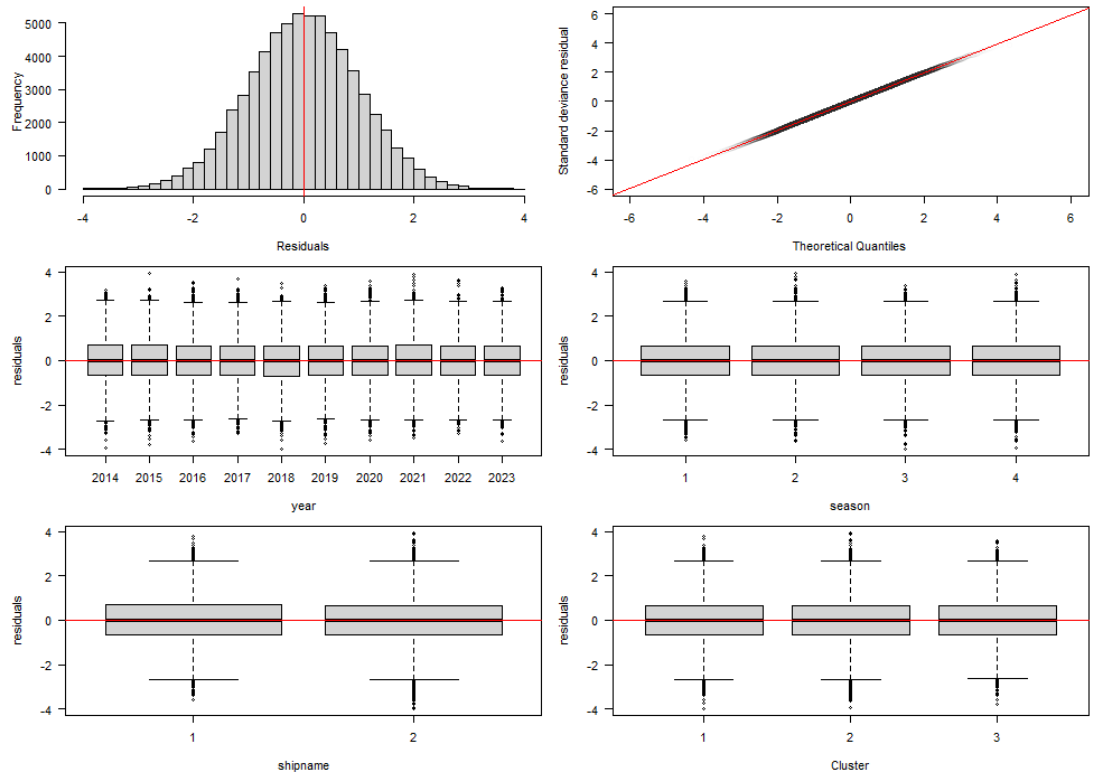

Figure 5.4 Diagnostic plots of goodness-of-fit for the most parsimonious model (Model-5) for white marlin in the Atlantic Ocean for P4 (2014-2023).

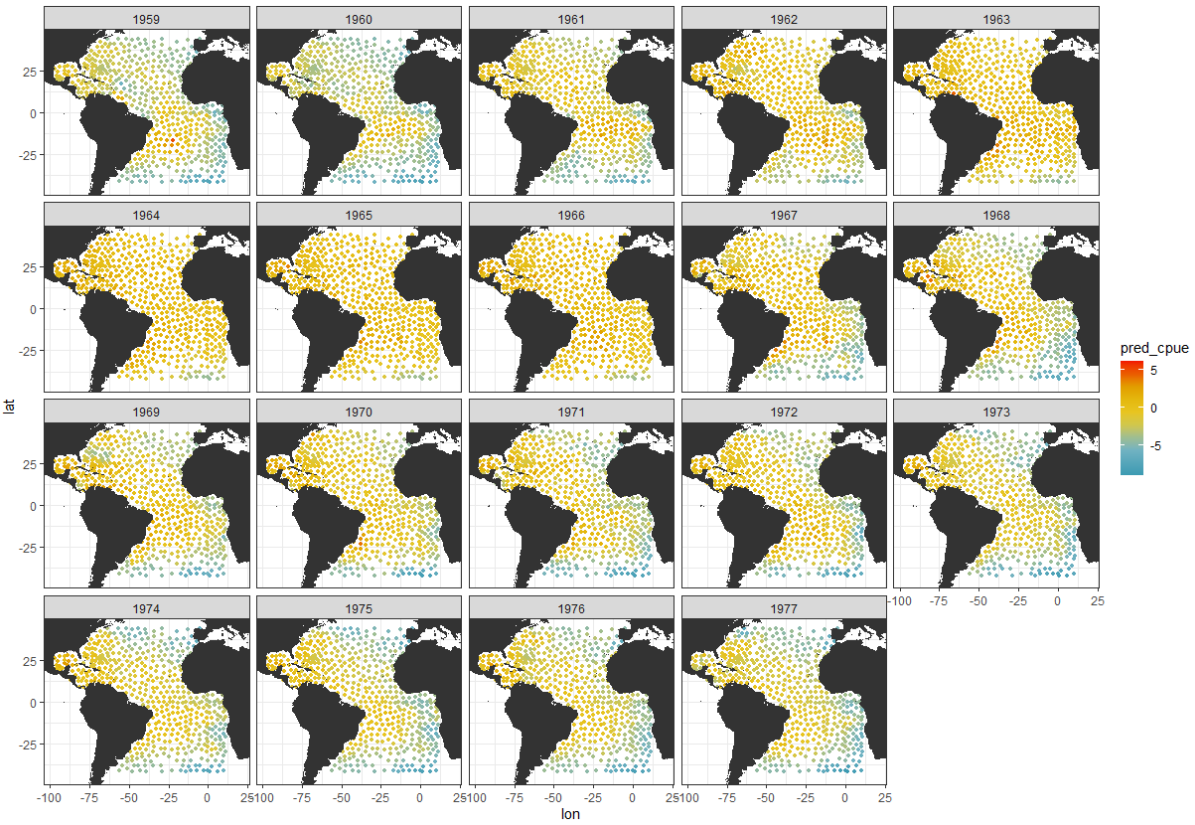

Figure 6.1 Annual spatial distribution of log-scaled estimated CPUE for white marlin in the Atlantic Ocean for P1 (1959-1977). Five hundred knots are given in the estimation of the standardized CPUE.

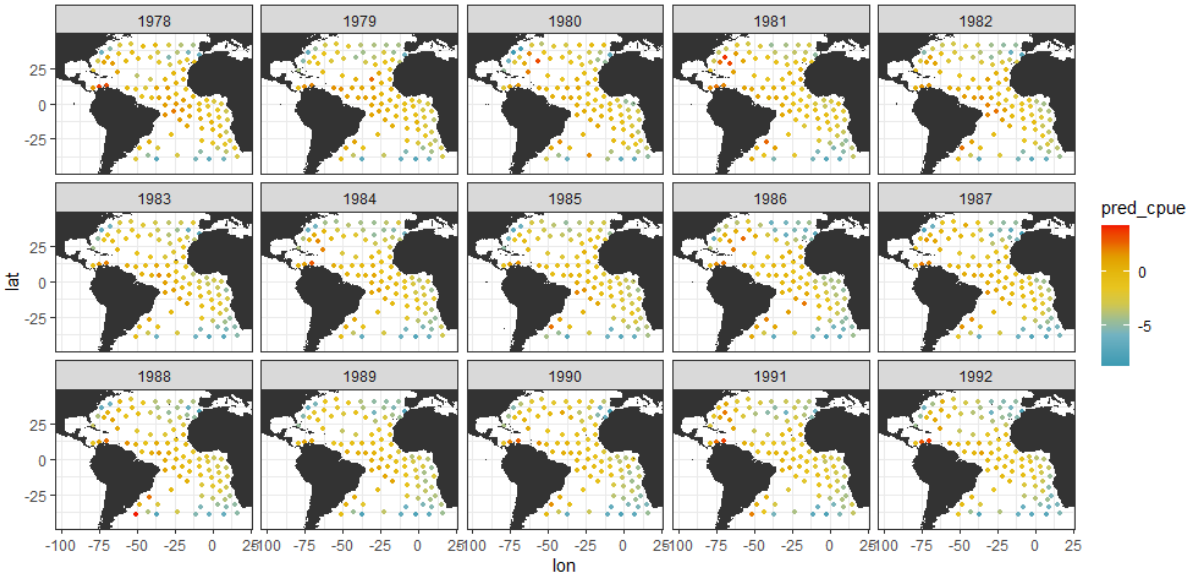

Figure 6.2 Annual spatial distribution of log-scaled estimated CPUE for white marlin in the Atlantic Ocean for P2 (1978-1992). A hundred knots are given in the estimation of the standardized CPUE.

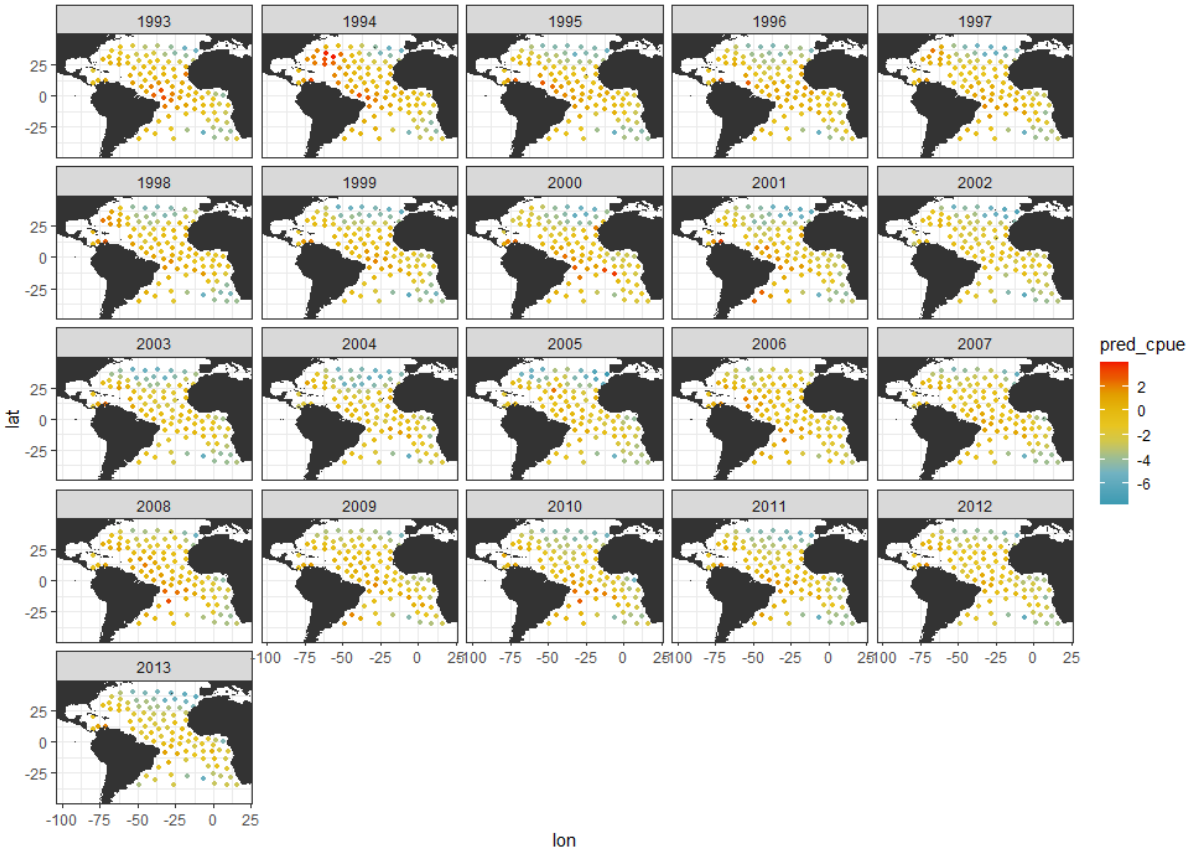

Figure 6.3 Annual spatial distribution of log-scaled estimated CPUE for white marlin in the Atlantic Ocean for P3 (1993-2013). A hundred knots are given in the estimation of the standardized CPUE.

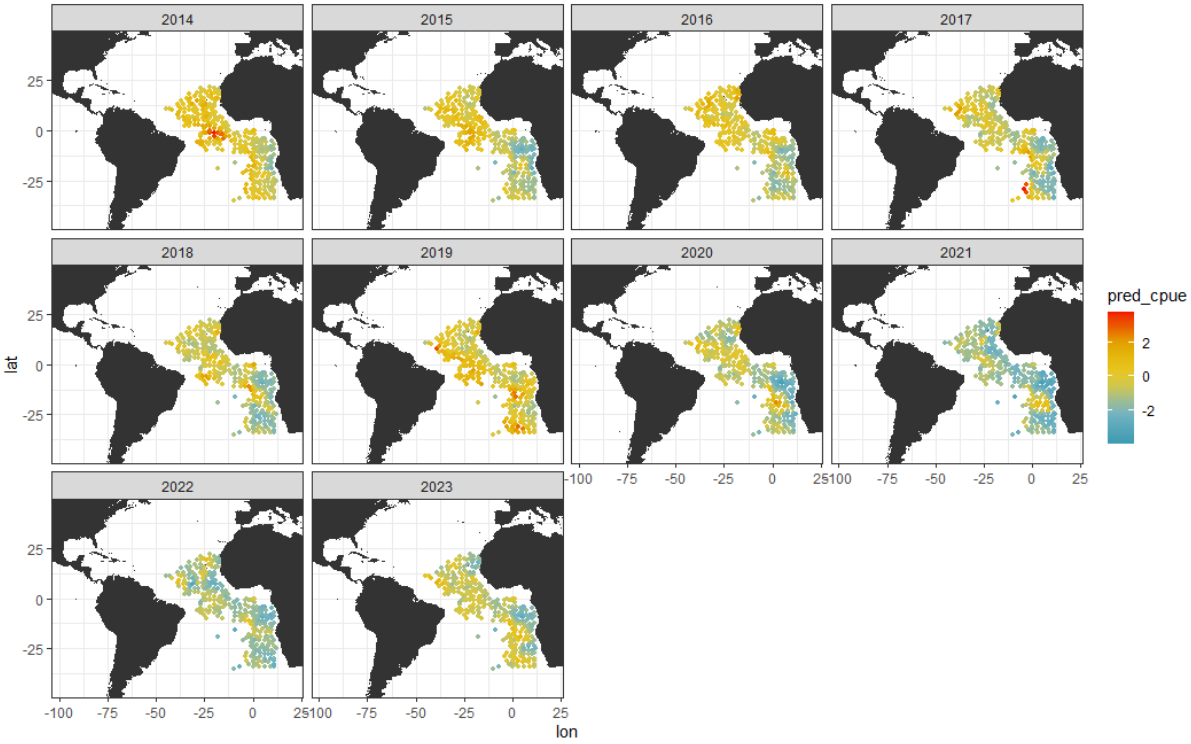

Figure 6.4 Annual spatial distribution of log-scaled estimated CPUE for white marlin in the Atlantic Ocean for P4 (2014-2023). Three hundred knots are given in the estimation of the standardized CPUE.

Appendix A

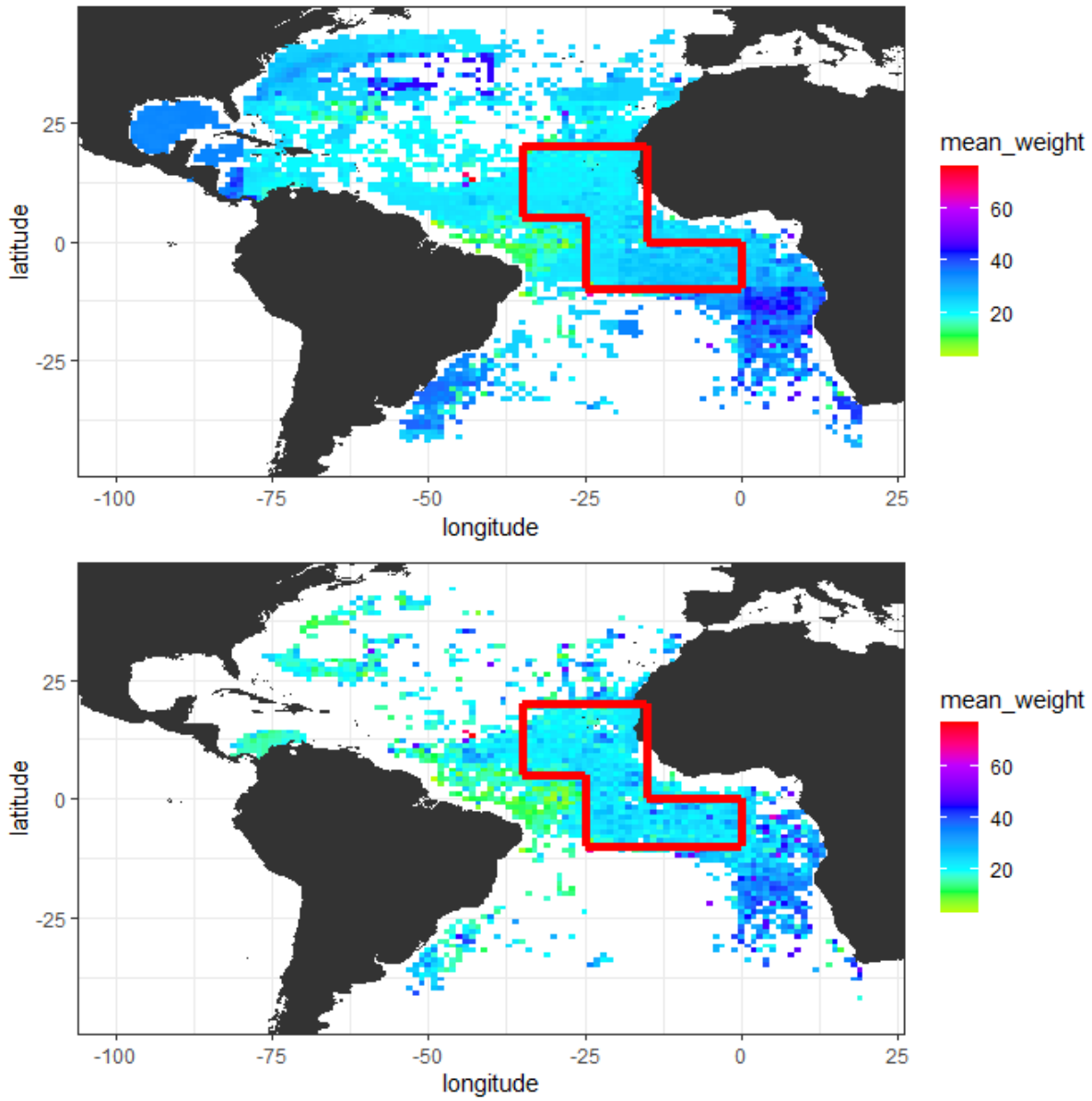

Figure A1. Spatial distribution of mean body weight (kg) for white marlin caught by Japanese longline fleets in the Atlantic Ocean for 1971-2023 (upper panel) and for 1994-2023 (lower panel). The data from the red polygonal frame area where the core area of semi-adult white marlin (about 30 kg) was used in the previous analysis (Ijima and Honda 2019). Data for white marlin weighing over 82 kg was removed based on the references of maximum weight for white marlin (Nakamura 1985).

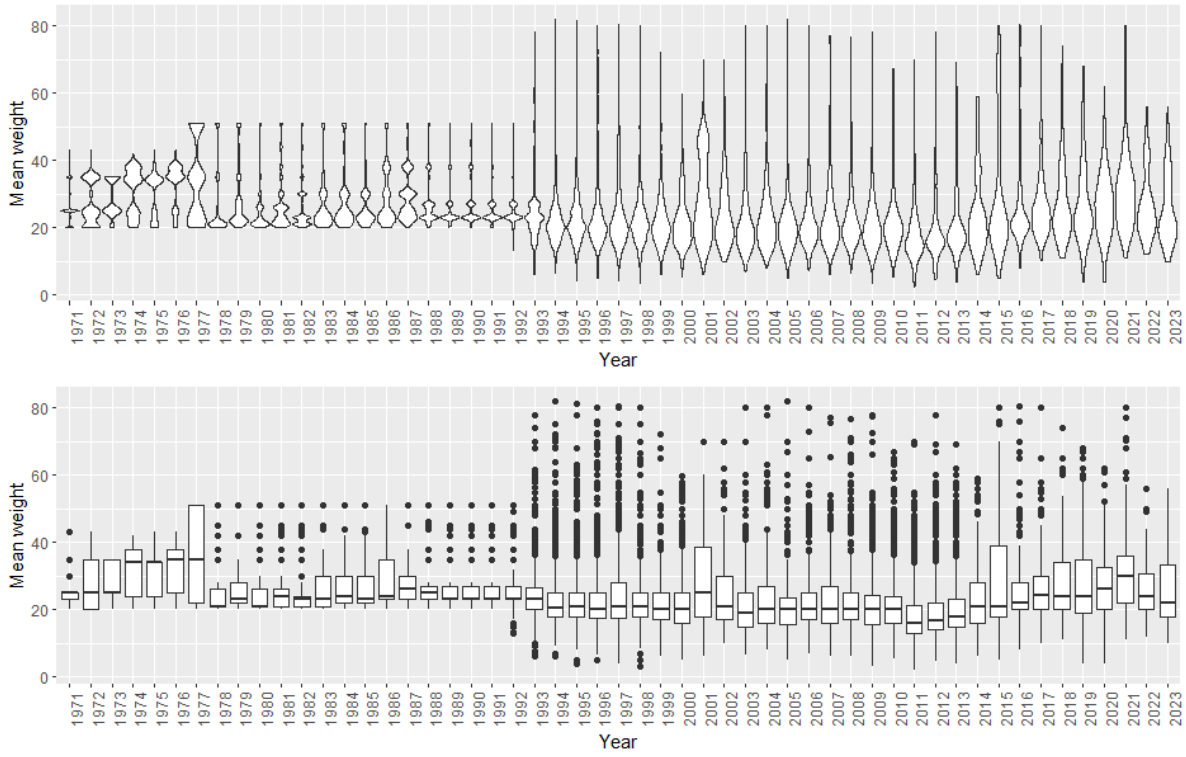

Figure A2. Annual changes in mean body weight (kg) for white marlin caught by Japanese longline fleets in the Atlantic Ocean. The upper panel denotes the violin-plot, and the lower panel denotes the boxplot. Data for white marlin weighing over 82 kg was removed based on the reference of maximum weight for white marlin (Nakamura 1985).

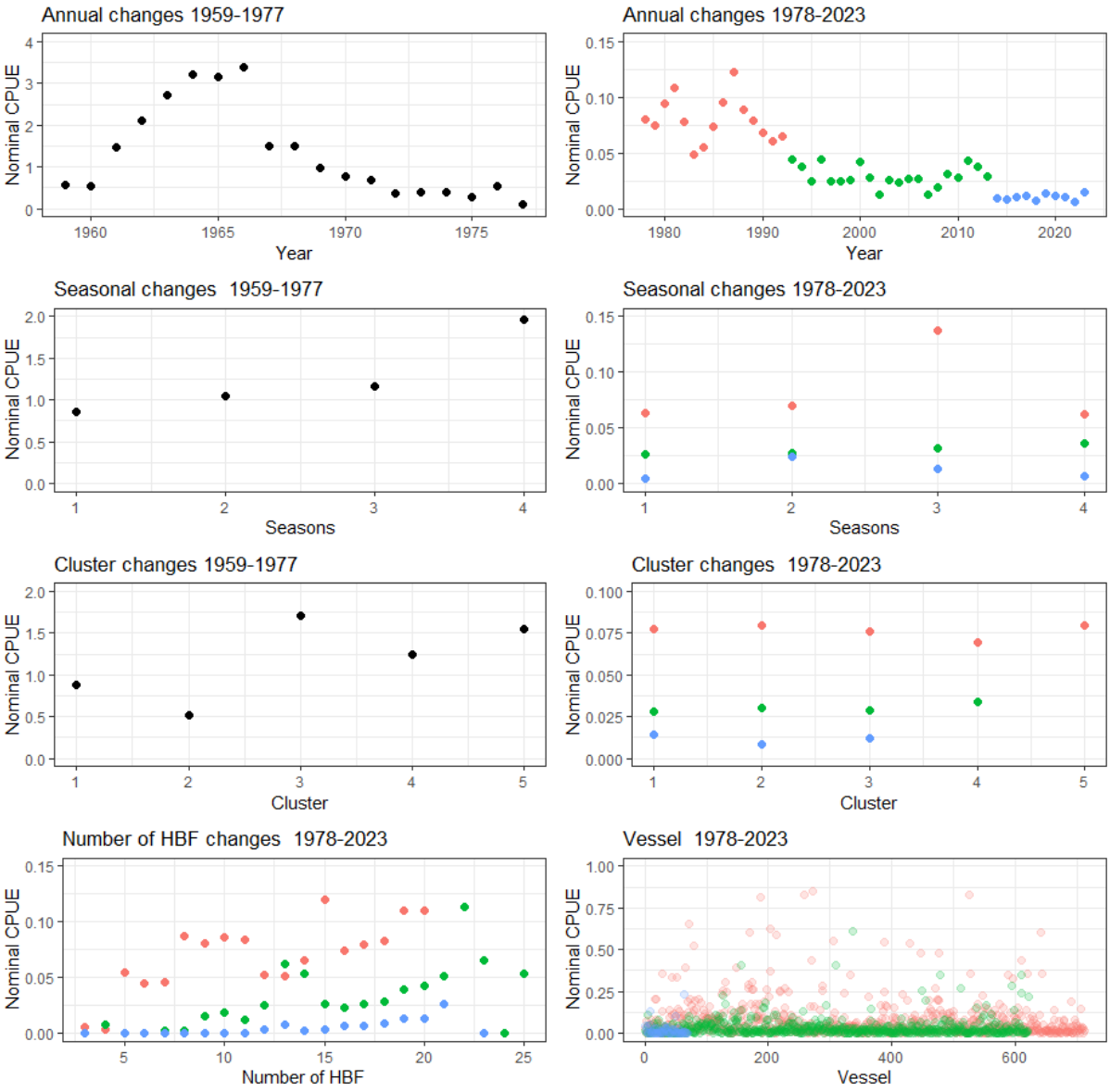

Figure A3. Changes in nominal CPUE (per 1000 hooks) by year, season, targeting cluster, number of hooks between floats (HBF), and vessel for four periods (P1: 1959-1977, P2: 1978-1992, P3: 1993-2013, and P4: 2014-2023) with the filtered datasets of white marlin in the Atlantic Ocean.

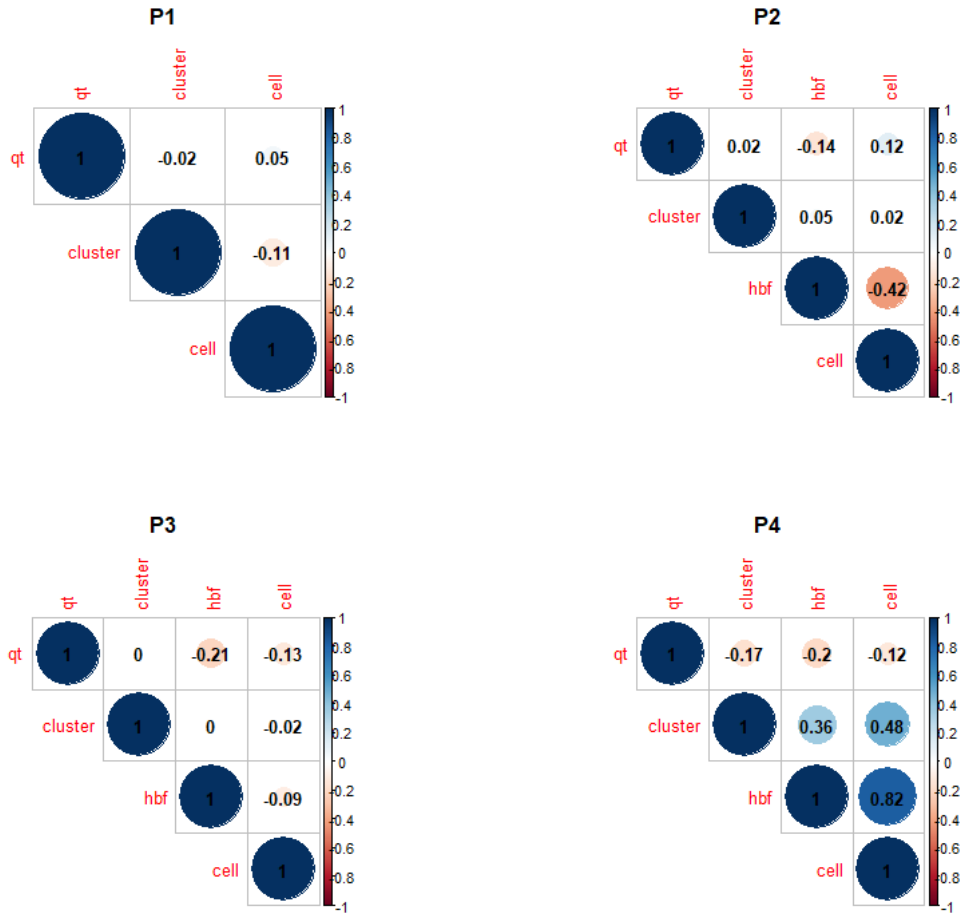

Figure A4. Correlation among quarters, number of hooks between floats (HBF), cell (station), and cluster for four periods (P1: 1959-1977, P2: 1978-1992, P3: 1993-2013, and P4: 2014-2023) using filtered datasets in the Atlantic Ocean.

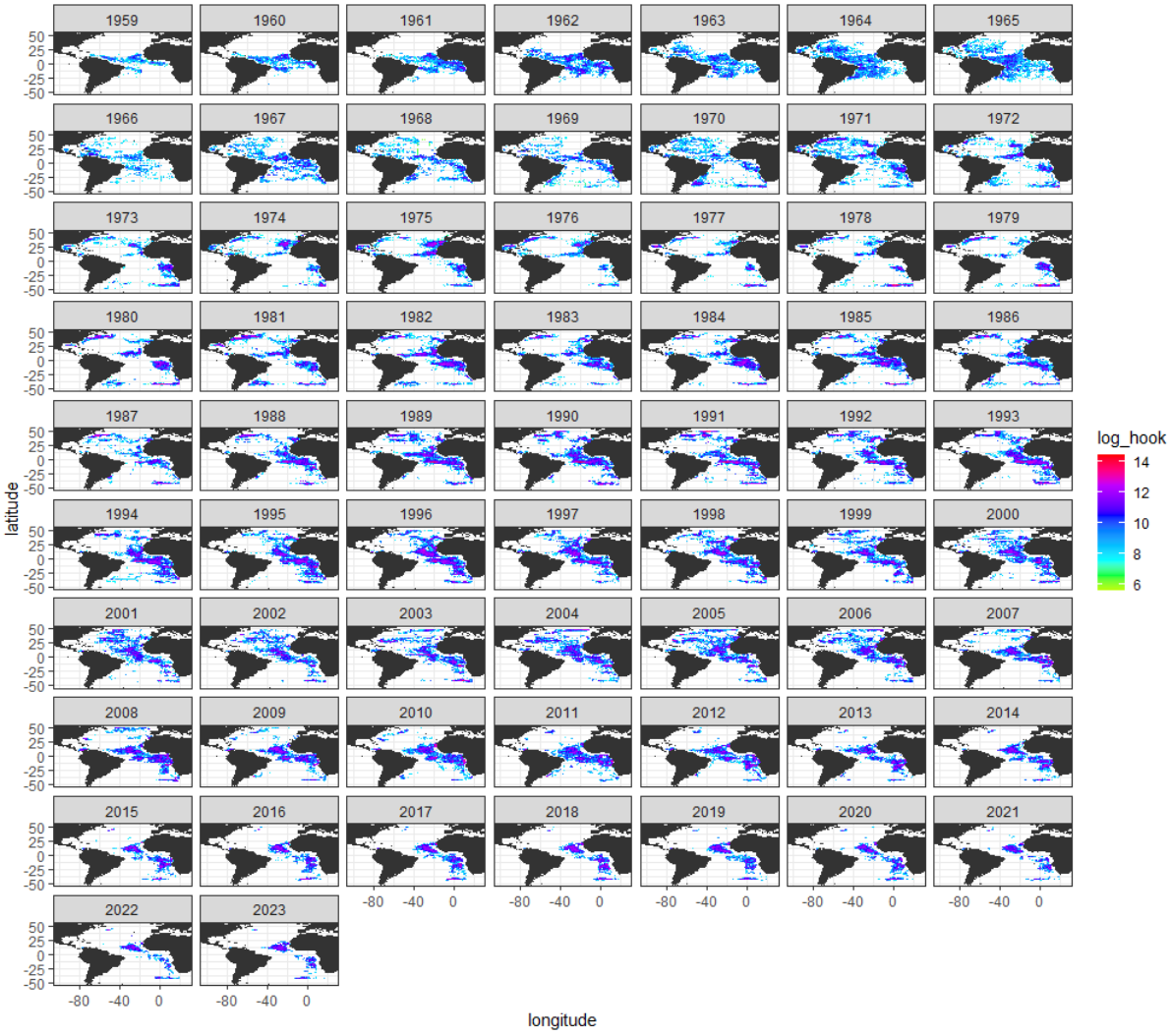

Figure A5. Annual changes in the spatial maps of fishing effort (log scale of the total number of hooks) by Japanese tuna longline fleets in the Atlantic Ocean from 1959 to 2023.

Figure A6. Annual changes in the species composition of catch numbers (upper panel) and the proportion of catch numbers (lower panel) for tunas and tuna-like species caught by the Japanese longline fishery in the Atlantic Ocean from 1959 to 2023.

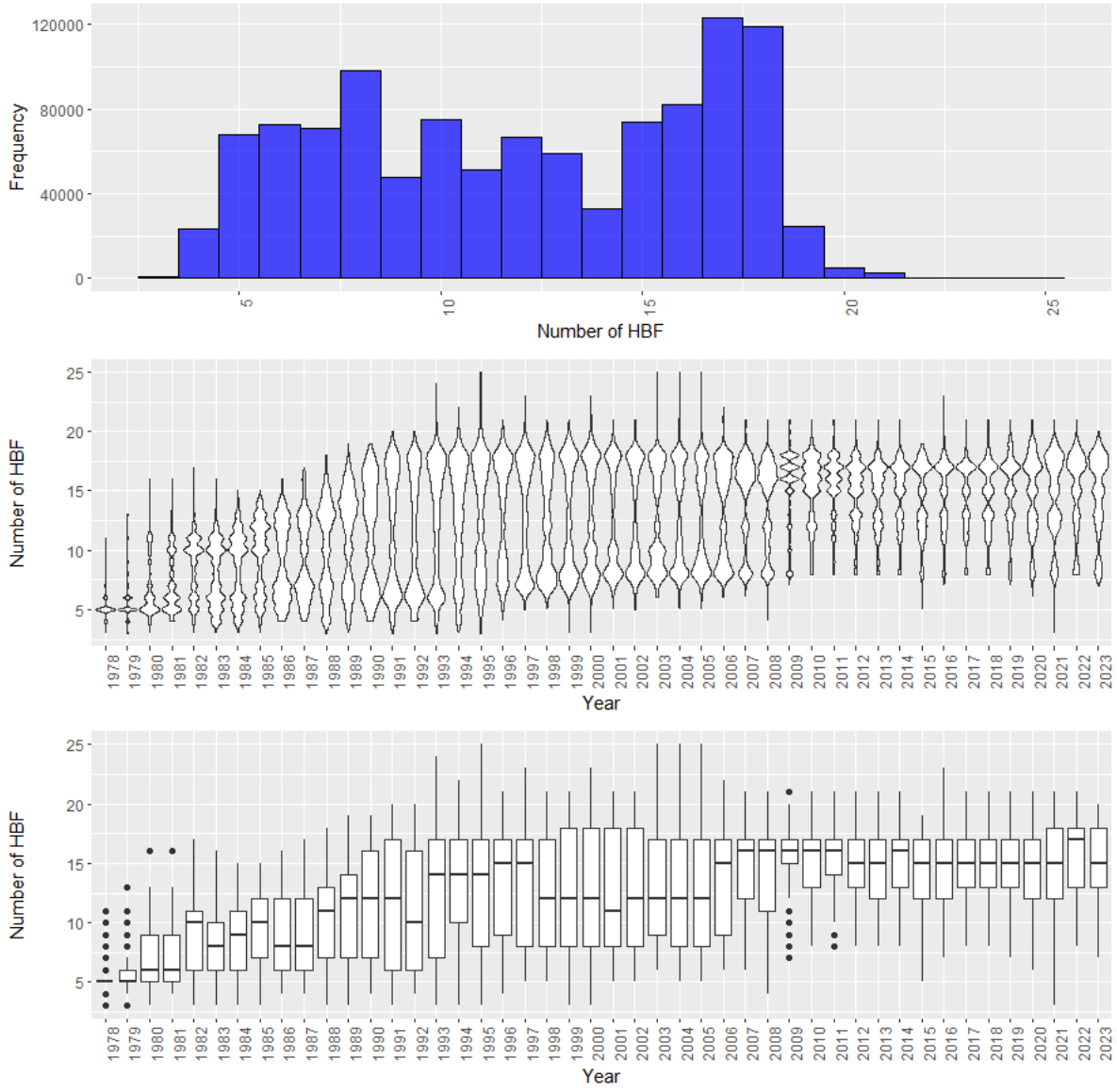

Figure A7. Frequency distribution of the number of hooks between floats (HBF) for Japanese tuna longline fleets in the Atlantic Ocean for 1978-2023 (upper panel), and the annual changes in HBF (middle panel shows a violin plot, and lower panel shows a boxplot).

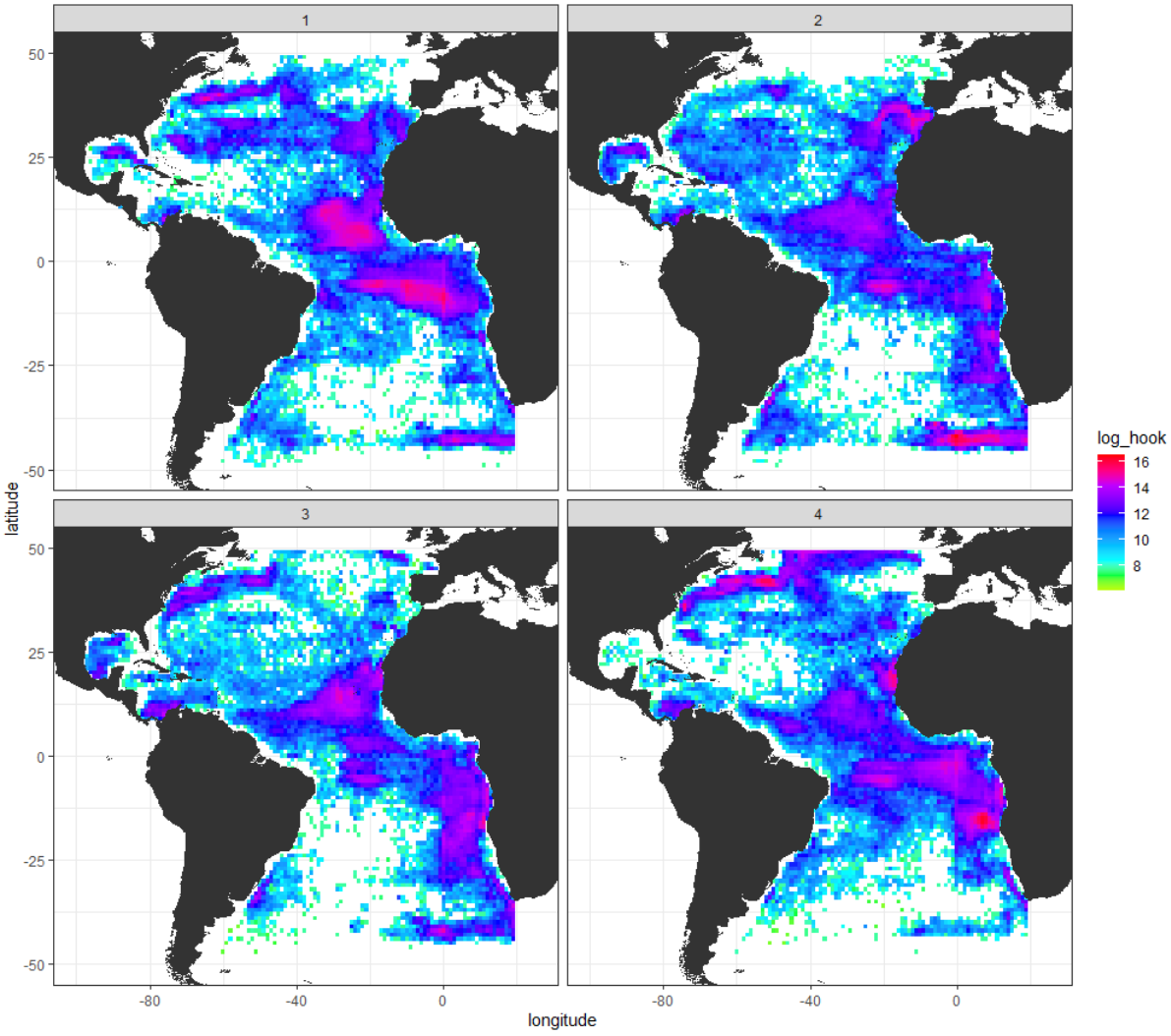

Figure A8. Seasonal changes in the spatial maps of fishing effort (log scale of the total number of hooks) by Japanese tuna longline fleets in the Atlantic Ocean between 1959 and 2023.